isvr Institute of Sound and Vibration Research

Nonlinear Forced Vibration of Beams by the Hierarchical Finite Element and Continuation Methods

R. Ribeiro and M. Petyt

ISVR Technical Memorandum 814

February 1997

University of Southampton

SCIENTIFIC PUBLICATIONS BY THE ISVR

Technical Reports are published to promote timely dissemination of research results by ISVR personnel. This medium permits more detailed presentation than is usually acceptable for scientific journals. Responsibility for both the content and any opinions expressed rests entirely with the author(s).

Technical Memoranda are produced to enable the early or preliminary release of information by ISVR personnel where such release is deemed to the appropriate. Information contained in these memoranda may be incomplete, or form part of a continuing programme; this should be borne in mind when using or quoting from these documents.

Contract Reports are produced to record the results of scientific work carried out for sponsors, under contract. The ISVR treats these reports as confidential to sponsors and does not make them available for general circulation. Individual sponsors may, however, authorize subsequent release of the material.

UNIVERSITY OF SOUTHAMPTON

INSTITUTE OF SOUND AND VIBRATION RESEARCH

STRUCTURAL DYNAMICS GROUP

Nonlinear Forced Vibration of Beams by the Hierarchical Finite Element and Continuation Methods

P. Ribeiro and M. Petyt

ISVR Technical Memorandum No. 814

February 1997

CONTENTS

NOTATION

A - area of the cross section of the beam

b - width of the beam

[C] - damping matrix

[D] - Jacobian of $\{F\}$

$|D|$ - determinant of [D]

E - Young's modulus

[E] - elastic matrix

{f} - vector of out-of plane shape functions

$\{F\}$ - vector of generalised external forces (amplitudes)

$\{\bar{F}\}$ - vector of generalised external forces (time dependent)

$\{F\}$ - vector of dynamic forces

h - length of the finite elements

h - thickness of the beam

I - second moment of area of the cross section of the beam

$[k_r]$ - diagonal matrix of modal stiffness

$[K1_b]$ - linear bending stiffness matrix

$[K1_p]$ - linear stretching stiffness matrix

[K2], [K3] and [K4] - components of nonlinear stiffness matrix

[Knl] - nonlinear stiffness matrix

L - length of the beam

$[m_r]$ - diagonal matrix of modal masses

[M] - mass matrix

$[M_b]$ - bending mass matrix

$[M_p]$ - in-plane mass matrix

$\lfloor N^w(x) \rfloor$ - row matrix of out-of-pl. sh. f.

p_i - number of in-plane shape functions

p_o - number of out-of-plane s. funct.

$\{q_p\}$ - in-plane displacement function

$\{q_w\}$ - transverse displacement function

r - radius of gyration

Re(cn) - real part of the complex number cn.

t - time

u - in-plane displacement

w - transverse displacement

$\{w_c\}$, $\{w_s\}$ - coefficients of cosine terms and sine terms, respectively

α - loss factor

β - damping factor

$\varepsilon_0^p, \varepsilon_0^b$ - linear membrane and bending strains

ε_L^p - geometrically nonlin. membrane strain

ε_x^0 - in-plane strain

$\{\varepsilon_1\}$ - linear strain

$\{\varepsilon_2\}$ - geometrically nonlinear strain

δW_{ex} - virtual work of the external forces

δW_v - virtual work of the internal forces

δW_{in} - virtual work of inertia forces

λ - characteristic exponent

ρ - mass density

ω - angular frequency

ω_{0j} - natural frequencies

$[\omega_{0j}^2]$ - diagonal matrix with squares of natural frequencies

ζ - Viscous damping ratio

1 - INTRODUCTION

The study of linear systems is much more straightforward and developed than the one of nonlinear systems. This can be attributed to the fact that the superposition principle, whereby the responses of a system to different excitations can be added linearly, is only applicable to linear systems. In real systems, due to large amplitudes of the excitation, small stiffness (usually resulting from requirements of slenderness or small weight of the structure) or excitation with a frequency in the neighbourhood of resonance frequencies, vibrations with large amplitudes can occur. In this case, the linear theories are not a good representation of the dynamic characteristics of the system.

Large amplitude vibrations take place, for example, in the aeronautical industry, where large excitations are applied to light, slender components such as beams and plates. Forced vibrations of beams and plates with geometrical nonlinearity, are described by an equation of the Duffing kind. The maximum amplitude of vibration is limited not only because of damping, but also because the stiffness increases with the amplitude of vibration. If the extremities of the beam are immovable, the nonlinearity is of the hardening spring type; therefore, the resonance frequencies increase with the amplitude of vibration.

A large amount of research has been done in the study of the nonlinear forced response of beams. In reference [28] one mode was used in Galerkin's method, to derive the equation of motion of a beam with fixed ends, excited by the periodic motion of its supporting base. The harmonic balance method (HBM) was used to solve this equation. The stability of the solutions was analysed solving a variational Hill-type equation. Bennet and Eisley [2] used a multiple mode Galerkin approach and the HBM, in an investigation of the nonlinear forced response of a clamped-clamped undamped beam, subjected to a concentrated harmonic force. Two and three degrees of freedom were considered. The response and stability were analysed. Using the Galerkin method and the perturbation procedure of multiple scales, Atluri [1] studied a beam with one end free to move longitudinally. The effect of midplane stretching was excluded and the effects of large curvature, longitudinal and rotatory inertia included. Calculated results showed that, with these conditions, the nonlinearity tends to be of

the softening type, because it is primarily determined by the longitudinal inertia. Takahashi [26] studied the steady-state response of an undamped non-linear clamped-clamped beam under periodic excitation. Due to symmetry conditions the system was simplified to a two-degree of freedom one. The Galerkin and the harmonic balance methods were used to derive the set of non-linear algebraic equations, which were solved by the Newton-Raphson method. Stability of the solution was studied by investigating the behaviour of a small perturbation to the steady state response. The resultant characteristic determinant was transformed to an eigenvalue problem.

In reference [15] a finite element formulation, including a harmonic force matrix, was presented for non-linear vibrations of undamped beam structures subjected to harmonic excitation. Longitudinal deformation and inertia were included in the formulation. For beams with an axially movable support it was found, as in [1], that the non-linearity can be of the soft spring type. In reference [11], a finite element method was applied together with the harmonic balance method, to determine the steady state response of beams and frames. The frequency response curves were constructed parametrically using the phase angle as a parameter.

For most boundary conditions, the shape and frequency of vibration change with the amplitude of vibration and, therefore, change during the cycle of vibration. In order to gain a better understanding of the variation of those parameters, in reference [14] the finite element equations of motion were derived in an incremental form in time. In every integral step, the system was assumed to be linear, thus, the mode superposition was valid and the orthogonality properties of the eigenmodes could be used to decouple the incremental equations of motion. The principal problem with this method, is the computational time required, mainly because for each nonlinear state of the structure natural frequencies and mode shapes have to be calculated. Moreover, the method only works for softening type nonlinearities, which are not at all common in beams with fixed ends and vibrating with large amplitudes.

Particularly in nonlinear analysis, more degrees of freedom represent additional complexity and more time needed to derive and solve the model. On the other hand, a reduced number of degrees of freedom can lead to considerable errors. The purpose of this report is to present a study of the forced vibration of beams with geometrical nonlinearity, by a method that allows the inclusion of higher order modes and damping,

without increasing excessively the number of degrees of freedom. This method is the hierarchical finite element method (HFEM).

In the HFEM hierarchichal shape functions are used [16] and, to make a better approximation, a higher order shape function is added, contrasting with the *h*-version of the finite element method where more elements would be introduced. The linear matrices possess the embedding property, meaning that the number of shape functions can be increased or decreased with the result that the associated element matrices for $n=n_1$ are always submatrices for $n=n_2$, $n_2 \geq n_1$. The existent nonlinear matrices of an approximation of lower order, n_1, can be used in the derivation of the nonlinear matrices of the improved approximation, n_2. This makes the construction of a new, more accurate model, potentially quicker in the HFEM method than in the *h*-version. Moreover, convergence properties of the HFEM tend to be better than the *h*-version ones [33].

Both perturbation methods, such as multiple scales and averaging [18], and the harmonic balance method have been used to find approximate solutions and their stability. Adding to its simplicity, the HBM has to its advantage the fact of not being restricted to weakly non-linear problems: even with large nonlinearities, very good results can be obtained if the right harmonics are used in the Fourier series. For smooth systems convergence to the exact solution is assured, which may not happen with perturbation methods [7]. Therefore, we are going to use the HBM to express the time variation of the solution.

For damped and forced nonlinear vibrations of a multi-degree of freedom system, the frequency response curves can have multi-valued regions, turning and bifurcation points. If the Newton method alone is applied, the solution will depend heavily on the initial guess and in the vicinity of resonance frequencies, when unstable solutions exist, convergence may be difficult to achieve. We are going to use a continuation method [12, 20, 23], which allows the complete description of the frequency response function (FRF) including determination of turning and bifurcation points with as much accuracy as desired, within the limits of the model and numerical errors.

When compared with the *h*-version of the finite element method, the disadvantage of the hierarchical finite element method is that if the shape functions

utilised are polynomials of high order, it might be difficult to integrate them accurately. The application of the HBM can be quite time demanding. Finally, in the continuation method, it is desirable to determine the Jacobian matrix involved in the process accurately. To do these operations, symbolic computation will be used [22].

2 - MATHEMATICAL MODEL

The beam considered is a thin beam made of isotropic linear material. The derivation of its HFEM model for free vibrations and the shape functions used were presented in [20]. One element was utilised. Here we shall introduce the damping matrix and the force vector present in the equations of motion of a beam under external excitation.

2.1 - DAMPING

Although some mathematical models do not include a damping term, in all real systems energy is dissipated and damping should be introduced in the model. With damping, the equations of motion for a multi-degree of freedom system take the form:

$$[M]\{\ddot{x}\} + [C]\{\dot{x}\} + [K]\{x\} + [KNL]\{x\} = \{\overline{F}\}. \qquad (2.1)$$

In a linear proportionally damped system, defined by having real normal modes, the equations of motion can be easily solved by first decoupling the equations via the use of normal modes. If these equations of motion can be decoupled, then there is no transfer of energy between principal forms of vibration, by the resistance forces. This was experimentally verified as plausible for a wide class of systems [31][1]. A sufficient condition [21], although not necessary [4], for the system to have real normal modes, is that the damping matrix may be expressed as a linear combination of the stiffness and mass matrices:

$$[C] = \alpha[K] + \beta[M] \qquad (2.2)$$

[1] Quoted in [3].

Very commonly the type of damping used is the viscous one. In this case, a term containing a first derivative of the displacement with respect to time is introduced in the differential equation of motion and the resistance forces are greatly dependent on velocity. If harmonic vibration is considered, it can be easily seen that the viscous damping model results in a dissipation of energy dependent on the frequency of vibration [19].

For a large variety of materials, however, experimental investigations show that the energy dissipated per cycle is not dependent on the frequency and is proportional to the square of the amplitude of vibration. This dissipation of energy is due to internal friction and is linked with the hysteresis phenomenon associated with cyclic stress in elastic materials [16]. The corresponding type of damping is called structural, hysteretic, material or viscoelastic. It can be represented by frequency dependent damping coefficients:

$$[C]=\frac{\alpha}{\omega}[K]+\frac{\beta}{\omega}[M] \tag{2.3}$$

2.2 - VECTOR OF EXTERNAL FORCES

The excitation forces can be expressed in terms of the actual force and the shape functions of the HFEM, by means of the virtual work performed by these forces. If $\overline{P}_j(t)$ represents a concentrated force acting at the point $x=x_j$ and $\overline{P}_d(x,t)$ represents a distributed force, the virtual work of the external forces is given by

$$\delta W_{ex}=\int_L\left[\overline{P}_j(t)\delta\left(x-x_j\right)+\overline{P}_d(x,t)\right]\delta w(x,t)dL \tag{2.4}$$

where $\delta\left(x-x_j\right)$ represents a spatial Dirac delta function given by

$$\begin{aligned}&\delta\left(x-x_j\right)=0 \qquad x\neq x_j\\ &\int_0^L\delta\left(x-x_j\right)dx=1\end{aligned} \tag{2.5}$$

so that $\overline{P}_j(t)\delta\left(x-x_j\right)$ has units of distributed force.

Assuming that the transverse displacement may be expressed as

$$w(x,t) = \lfloor q_w(t) \rfloor \{N^w(x)\}, \tag{2.6}$$

we have

$$\delta W_{ex} = \lfloor \delta q_w(t) \rfloor \left(\int_L \bar{P}_d(x,t) \{N^w(x)\} dL + \bar{P}_j(t) \{N^w(x_j)\} \right) \tag{2.7}$$

So the generalised forces are

$$\{\bar{F}\} = \left(\int_L \bar{P}_d(x,t) \{N^w(x)\} dL + \bar{P}_j(t) \{N^w(x_j)\} \right). \tag{2.8}$$

2.3 - EQUATIONS OF MOTION

Due to the presence of external and dissipative forces, the system is a nonconservative one. In the absence of damping, applying the principle of virtual work, we have

$$\delta W_{ex} - \delta W_V - \delta W_d = \delta W_{in} \tag{2.9}$$

δW_{ex} was derived in the previous section, δW_V and δW_{in} were derived in reference [20].

The damping considered will be of the hysteretic type and the matrix which represents it will be approximated by a scalar times the mass matrix. Considering that damping in the beam results only from the action of the linear axial and bending strains, and that only transverse forces are applied, we have the following equations of motion:

$$\begin{bmatrix} M_p & 0 \\ 0 & M_b \end{bmatrix} \begin{Bmatrix} \ddot{q}_p \\ \ddot{q}_w \end{Bmatrix} + \begin{bmatrix} \frac{\beta_p}{\omega} M_p & 0 \\ 0 & \frac{\beta}{\omega} M_b \end{bmatrix} \begin{Bmatrix} \dot{q}_p \\ \dot{q}_w \end{Bmatrix} + \left(\begin{bmatrix} K1_p & 0 \\ 0 & K1_b \end{bmatrix} + \begin{bmatrix} 0 & K2 \\ K3 & K4 \end{bmatrix} \right) \begin{Bmatrix} q_p \\ q_w \end{Bmatrix} = \begin{Bmatrix} 0 \\ \bar{F} \end{Bmatrix} \tag{2.10}$$

which can be partitioned into two equations:

$$[M_p] \{\ddot{q}_p\} + \frac{\beta_p}{\omega} [M_p] \{\dot{q}_p\} + [K1_p] \{q_p\} + [K2] \{q_w\} = 0 \tag{2.11}$$

$$[M_b]\{\ddot{q}_w\}+\frac{\beta}{\omega}[M_b]\{\dot{q}_w\}+[K3]\{q_p\}+([Kl_b]+[K4])\{q_w\}=\{\bar{F}\} \quad (2.12)$$

The in-plane inertia can be neglected for slender beams [5] and the damping contribution due to the axial stress is generally negligible compared to that due to the bending stress [17]. With these approximations, we can simplify the equations of motion to obtain:

$$[M_b]\{\ddot{q}_w\}+\frac{\beta}{\omega}[M_b]\{\dot{q}_w\}+[Kl_b]\{q_w\}+[Knl]\{q_w\}=\{\bar{F}\}, \quad (2.13)$$

$$[Knl]=[K4]-2[K2]^T[Kl_p]^{-1}[K2]. \quad (2.14)$$

$$[K3]=2[K2]^T \text{ from reference [6].} \quad (2.15)$$

If the external excitation is harmonic, then the steady state response, $\{q_w(t)\}$, may be expressed in a first approximation as:

$$\{q_w(t)\}=\{w_c\}\cos(\omega t)+\{w_s\}\sin(\omega t) \quad (2.16)$$

We are going to insert this equation into the equations of motion and apply the harmonic balance method. This method can be easily implemented in a program produced with the symbolic manipulator *Maple* [29]. For that we use the command

trign:=readlib('trig/reduce'):

where *readlib* is a *Maple* library function, to replace all nonlinear trigonometric functions by linear ones and the command *coeff* to select the terms in cos(ωt) and sin(ωt). In this way, we obtain equations of motion of the form:

$$-\omega^2\begin{bmatrix}M_b & 0\\ 0 & M_b\end{bmatrix}\begin{Bmatrix}w_c\\ w_s\end{Bmatrix}+\begin{bmatrix}0 & \beta M_b\\ -\beta M_b & 0\end{bmatrix}\begin{Bmatrix}w_c\\ w_s\end{Bmatrix}+\begin{bmatrix}Kl_b & 0\\ 0 & Kl_b\end{bmatrix}\begin{Bmatrix}w_c\\ w_s\end{Bmatrix}+$$
$$\begin{bmatrix}\frac{3}{4}KNL1+\frac{1}{4}KNL3 & \frac{1}{4}KNL2\\ \frac{1}{4}KNL2 & \frac{1}{4}KNL1+\frac{3}{4}KNL3\end{bmatrix}\begin{Bmatrix}w_c\\ w_s\end{Bmatrix}=\{F\} \quad (2.17)$$

The matrices KNL1, KNL2 and KNL3 have the form of [Knl] in (2.14), where KNL1 is a function of $\{w_c\}$ only, KNL2 a function of both $\{w_c\}$ and $\{w_s\}$ and KNL3 a function of $\{w_s\}$ only [2]. M_b, $K1_b$, KNL1, KNL2 and KNL3 are symmetric matrices.

To solve this system of equations Newton's method was used for nonresonant frequencies. In the vicinity of resonance frequencies it is difficult to obtain convergence by the Newton method and a continuation method was used. The procedure is similar to the one utilised in [20], with

$$\{F\}=\left(-\omega^2\begin{bmatrix} M_b & 0 \\ 0 & M_b \end{bmatrix}+\begin{bmatrix} 0 & \beta M_b \\ -\beta M_b & 0 \end{bmatrix}+\begin{bmatrix} K1_b & 0 \\ 0 & K1_b \end{bmatrix}\right.$$

$$\left.\begin{bmatrix} \frac{3}{4}KNL1+\frac{1}{4}KNL3 & \frac{1}{4}KNL2 \\ \frac{1}{4}KNL2 & \frac{1}{4}KNL1+\frac{3}{4}KNL3 \end{bmatrix}\right)\begin{Bmatrix} w_c \\ w_s \end{Bmatrix}-\{F\}=\{0\}^3 \qquad (2.18)$$

3 - STUDY OF THE STABILITY OF THE SOLUTIONS

3.1 - INTRODUCTION

The study of the stability of an equilibrium solution is concerned with what happens if a system is slightly disturbed from it. A perturbation near an unstable equilibrium condition leads to a departure from this condition and the inverse occurs near a stable equilibrium condition. In a nonlinear system more than a single equilibrium condition may appear and the question of stability is particularly important, because only stable equilibrium solutions exist actually, whereas an unstable one can not be maintained.

We shall study the problem of local stability of the harmonic solution

$$\{q_w\}=\{w_c\}\cos(\omega t)+\{w_s\}\sin(\omega t), \qquad (3.1)$$

---

[2] With this formulation, KNL2 must be calculated using $2\lfloor N_x^w\rfloor\{w_c\}\lfloor N_x^w\rfloor\{w_s\}$, otherwise $\frac{1}{2}KNL2$ shall be considered instead of $\frac{1}{4}$ KNL2. Note that the matrix [Knl] is an explicit function of time, whilst KNL1, KNL2 and KNL3 are not.

[3] In [20], the vector of dynamic forces is represented by {F} instead of $\{F\}$.

of equation

$$[M_b]\{\ddot{q}_w\}+\frac{\beta}{\omega}[M_b]\{\dot{q}_w\}+[Kl_b]\{q_w\}+[Knl]\{q_w\}=\{F\}\cos(\omega t), \quad (3.2)$$

$$[Knl]=[K4]-2[K2]^T[Kl_p]^{-1}[K2], \quad (3.3)$$

by Floquet's theory.

To do this we add a small disturbance to the steady state solution

$$\{\tilde{q}\}=\{q_w\}+\{\delta q_w\} \quad (3.4)$$

or

$$\tilde{q}_{w_i}(t)=q_{w_i}(t)+\delta q_{w_i}(t), \qquad i=1, 2, \ldots, p_o, \quad (3.5)$$

and study how the variation of the solution evolves. If $\{\delta q_w\}$ dies out with time then $\{q_w\}$ is stable, if it grows then $\{q_w\}$ is unstable.

Inserting the disturbed solution (3.5) into equation (3.2), expanding nonlinear terms into Taylor series around $\{q_w\}$ and ignoring terms of order higher then $\{\delta q_w\}$, we obtain the variational equation:

$$[M_b]\{\delta\ddot{q}_w\}+\frac{\beta}{\omega}[M_b]\{\delta\dot{q}_w\}+[Kl_b]\{\delta q_w\}+\frac{\partial([Knl]\{q_w\})}{\partial\{q_w\}}\{\delta q_w\}=\{0\}. \quad (3.6)$$

The coefficients $\frac{\partial([Knl]\{q_w\})}{\partial\{q_w\}}$ are periodic functions of time. With symbolic manipulation, they can easily be expanded in a Fourier series (note that if the solution is of the form (3.1), there is no approximation in this step):

$$\frac{\partial([Knl]\{q_w\})}{\partial\{q_w\}}=[[p_1]+[p_2]\cos(2\omega t)+[p_3]\sin(2\omega t)]. \quad (3.7)$$

$$[p_1]=\frac{1}{T}\int_0^T\frac{\partial}{\partial q_w}([Knl]\{q_w\})\,dt$$

$$[p_2]=\frac{2}{T}\int_0^T\frac{\partial}{\partial q_w}([Knl]\{q_w\})\cos(2\omega t)dt$$

$$[p_3]=\frac{2}{T}\int_0^T \frac{\partial}{\partial q_w}\left([Knl]\{q_w\}\right)\sin(2\omega t)dt$$

So [p1], [p2] and [p3] are the coefficients of Fourier of $\frac{\partial([Knl]\{q_w\})}{\partial\{q_w\}}$. They are functions of $\{q_w\}$.

Inserting equation (3.7) into the variational equations (3.6), we have

$$[M_b]\{\delta\ddot{q}_w\}+\frac{\beta}{\omega}[M_b]\{\delta\dot{q}_w\}+[Kl_b]\{\delta q_w\}+[[p_1]+[p_2]\cos(2\omega t) +[p_3]\sin(2\omega t)]\{\delta q_w\}=\{0\} \quad (3.8)$$

which forms a system of Hill's equations. The general theory of Hill's equations says that the stable and unstable regions alternate along the frequency axis and that the unstable regions appear in the neighbourhood of the following frequency values [24]

$$\text{I. } \omega \cong \frac{\omega_{0i}}{k},\ k=1, 3, 5 \ldots \text{ or } k=2, 4, 6\ldots \quad (3.9)$$

$$\text{II. } \omega \cong \frac{\omega_{0i} \pm \omega_{0s}}{k},\ k=1, 2, 3\ldots;\ i,s=1, 2, \ldots \quad (3.10)$$

where ω_{0i} are the natural frequencies of the system

$$[M_b]\{\delta\ddot{q}_w\}+\frac{\beta}{\omega}[M_b]\{\delta\dot{q}_w\}+[[Kl_b]+[p_1]]\{\delta q_w\}=\{0\}$$

For small amplitudes $[p_1]$ is negligible and ω_{0i} are equal to the linear natural frequencies of vibration of the beam. If k=1 in (3.9), we have simple order instabilities; if $k > 1$ the instability is of higher order. Note that higher order instabilities only play a meaningful role for very large amplitudes of excitation [24]. From frequencies (3.10) combination type of instabilities develop.

Next, we will present two methods to solve (3.8) and obtain the evolution of $\{\delta q\}$ with time. The first one is based on the HBM and the second is based on a perturbation procedure. Two different forms of the assumed harmonic solution will be tried when applying the HBM. Finally, it is shown that important conclusions about the stability of the solution can be deducted from the determinant of the Jacobian of $\{F\}$.

The study of stability due to combination resonances can be carried out either using perturbation methods, involving the small parameter concept [10, 24], or by assuming that the solution on the boundary of the combination resonance is a two-harmonic components function of time for all the co-ordinates [25]. As the study of combination resonances and their stability is the subject of a future work, only the stability of the solution in the neighbourhood of simple resonances will be verified.

3.2 - HARMONIC BALANCE METHOD

3.2.1 - Bolotin's solution [3] [4]

To uncouple the linear part of the variational equations, we will change into modal coordinates of the linear system. These are defined by

$$\{\delta q_w\} = [B]\{\delta\xi\} \tag{3.11}$$

where $[B]$ is the modal matrix of

$$[M_b]\{\delta\ddot{q}_w\} + [Kl_b]\{\delta q_w\} = \{0\}. \tag{3.12}$$

$[B]$ satisfies the relation

$$[B]^T[M_b][B] = [m_r] \tag{3.13}$$

$$[B]^T[Kl_b][B] = [k_r]. \tag{3.14}$$

If we divide each modal vector by the square root of the correspondent modal mass, m_r, we normalise them so that

$$[B]^T[M_b][B] = [I], \tag{3.15}$$

$$[B]^T[Kl_b][B] = [\omega_{0j}^2]. \tag{3.16}$$

Multiplying equations (3.8) by $[B]^T$ and using modal coordinates, we arrive at:

[4] Both this and the next section were named after two well known authors, from whose books the methods were taken from.

$$\{\delta\ddot{\xi}\}+\frac{\beta}{\omega}[I]\{\delta\dot{\xi}\}+[\omega_{0j}^{2}]\{\delta\xi\}+[B]^{T}([p_1]+[p_2]\cos(2\omega t)+[p_3]\sin(2\omega t))[B]\{\delta\xi\}=\{0\} \tag{3.17}$$

This is a system of extended coupled Hill's equations. The first derivative term in equation (3.17) can be eliminated by introducing a new vector of variables

$$\{\delta\xi\}=e^{-\frac{1}{2}\frac{\beta}{\omega}[I]t}\{\delta\bar{\xi}\}, \tag{3.18}$$

obtaining, because matrix $e^{-\frac{1}{2}\frac{\beta}{\omega}[I]t}$ commutes with any other matrix,

$$e^{-\frac{1}{2}\frac{\beta}{\omega}[I]}\left(\{\delta\ddot{\bar{\xi}}\}+\left([\omega_{0j}^{2}]-\frac{1}{4}\left(\frac{\beta}{\omega}\right)^{2}[I]+[B]^{T}([p_1]+[p_2]\cos(2\omega t)+[p_3]\sin(2\omega t))[B]\right)\{\delta\bar{\xi}\}\right)=\{0\} \tag{3.19}$$

and since $e^{-\frac{1}{2}\frac{\beta}{\omega}[I]t}$ is nonsingular, we have

$$\{\delta\ddot{\bar{\xi}}\}+\left([\omega_{0j}^{2}]-\frac{1}{4}\left(\frac{\beta}{\omega}\right)^{2}[I]+[B]^{T}([p_1]+[p_2]\cos(2\omega t)+[p_3]\sin(2\omega t))[B]\right)\{\delta\bar{\xi}\}=\{0\} \tag{3.20}$$

Inserting a solution of the following form [3, page 214], [26]

$$\{\delta\bar{\xi}\}=e^{\lambda t}\left\{\frac{1}{2}\{b_0\}+\sum_{k=1}^{\infty}(\{a_k\}\sin(2k\omega t)+\{b_k\}\cos(2k\omega t))\right\} \tag{3.21}$$

in equation (3.20), we obtain

$$\lambda^{2}\left\{\frac{1}{2}\{b_0\}+\sum_{k=1}^{\infty}(\{a_k\}\sin(2k\omega t)+\{b_k\}\cos(2k\omega t))\right\}+2\lambda\sum_{k=1}^{\infty}2k\omega(\{a_k\}\cos(2k\omega t)-\{b_k\}\sin(2k\omega t))$$
$$+\sum_{k=1}^{\infty}(2k\omega)^{2}(-\{a_k\}\sin(2k\omega t)-\{b_k\}\cos(2k\omega t))+([\Lambda 1]+[\Lambda 2]\cos(2\omega t)+[\Lambda 3]\sin(2\omega t))$$
$$\left\{\frac{1}{2}\{b_0\}+\sum_{k=1}^{\infty}(\{a_k\}\sin(2k\omega t)+\{b_k\}\cos(2k\omega t))\right\}=\{0\} \tag{3.22}$$

$$[\Lambda 1]=[\omega_{0j}^{2}]-\frac{1}{4}\left(\frac{\beta}{\omega}\right)^{2}[I]+[B]^{T}[p1][B], \tag{3.23}$$

$$[\Lambda 2]=[B]^{T}[p2][B], \tag{3.24}$$

$$[\Lambda 3] = [B]^T [p3][B]. \tag{3.25}$$

For $\mathrm{Re}(\lambda)\neq 0$[5], solutions (3.21) are not periodic due to the presence of the factor $e^{\lambda t}$. It should be noted that the simplification (3.20) was only possible because we are working with a damping matrix which, after transformation into modal coordinates, is equal to a scalar times the identity matrix. This type of proportional damping, simplifies the study of the stability. If other kinds of damping are used, reflecting different damping coefficients for different modes, it is possible to make a study of stability similar to this one. In this case transformation (3.18) is not used and extra terms must be introduced in (3.21) [27].

Again using Maple commands, we divide the coefficients of each harmonic in equation (3.22) and, with the resulting equations, we construct a system of the form:

$$\left(\lambda^2[M_2] + \lambda[M_1] + [M_0]\right)\{X\} = \{0\}, \tag{3.26}$$

where $\{X\}$ is a vector formed by $\{a_k\}$, $\{b_0\}$, $\{b_k\}$.

To determine the characteristic exponents we transform this system into [26]

$$\begin{bmatrix} 0 & [I] \\ -[M_2]^{-1}[M_0] & -[M_2]^{-1}[M_1] \end{bmatrix} \begin{Bmatrix} X \\ \Gamma \end{Bmatrix} = \lambda \begin{Bmatrix} X \\ \Gamma \end{Bmatrix}, \tag{3.27}$$

So the values of λ, called characteristic exponents, are the eigenvalues of the double size matrix in the previous equation. Bearing in mind that it is the stability for the variable $\{\delta\xi\}$ in which we are interested, we substitute equation (3.21) into equation (3.18) to obtain

$$\{\delta\xi\} = e^{\left(\lambda - \frac{1}{2}\frac{\beta}{\omega}\right)t} \left\{ \frac{1}{2}\{b_0\} + \sum_{k=1}^{\infty} \left(\{a_k\}\sin(2k\omega t) + \{b_k\}\cos(2k\omega t) \right) \right\}. \tag{3.28}$$

If

$$\mathrm{Re}\left(\lambda_r - \frac{1}{2}\frac{\beta}{\omega}\right) > 0 \tag{3.29}$$

for any λ_r, then the solution is unstable, otherwise it is stable.

[5] $\mathrm{Re}(\lambda)$ designates the real part of λ.

3.2.2 - Hayashi's solution [9]

On the stability limit the solution of (3.20) has period T or 2T, where T is the period of the periodic function in equation (3.20):

$$T=\frac{\pi}{\omega}. \tag{3.30}$$

Two solutions with the same period confine the region of instability and two solutions with different periods confine the regions of stability [3, 9]. On this basis, we can find the regions of instability of an undamped system, determining under which conditions the differential equations have periodic solutions with period T or 2T. To find the solutions with period T a series of the form

$$\left\{\delta\bar{\xi}\right\} = \sum_{k=1,3,5}^{\infty}\left(\left\{a_k\right\}\sin(k\omega t) + \left\{b_k\right\}\cos(k\omega t)\right) \tag{3.31}$$

is considered. To find the solutions with period 2T we insert a series of the form

$$\left\{\delta\bar{\xi}\right\} = \frac{1}{2}\left\{b_0\right\} + \sum_{k=2,4,6}^{\infty}\left(\left\{a_k\right\}\sin(k\omega t) + \left\{b_k\right\}\cos(k\omega t)\right) \tag{3.32}$$

in the variational equations.

In [9] it is sugested to use, instead of (3.21), series similar to the last ones multiplied by an exponential term with the characteristic exponents. The series

$$\left\{\delta\bar{\xi}\right\} = e^{\lambda t}\sum_{k=1,3,5}^{\infty}\left(\left\{a_k\right\}\sin(k\omega t) + \left\{b_k\right\}\cos(k\omega t)\right), \tag{3.33}$$

will allow us to determine unstable regions of odd order and with the series

$$\left\{\delta\bar{\xi}\right\} = e^{\lambda t}\left(\frac{1}{2}\left\{b_0\right\} + \sum_{k=2,4,6}^{\infty}\left(\left\{a_k\right\}\sin(k\omega t) + \left\{b_k\right\}\cos(k\omega t)\right)\right) \tag{3.34}$$

we can determine unstable regions of even order.

To determine simple instabilities of first order, we assume a solution of the form

$$\left\{\delta\bar{\xi}\right\} = e^{\lambda t}\left(\left\{b_1\right\}\cos(\omega t) + \left\{a_1\right\}\sin(\omega t)\right). \tag{3.35}$$

which has the advantage of being of the same type as the steady state response. Then a method similar to the one presented in the previous section is applied to determine the characteristic exponents. A comprehensive derivation of the matrices [M2], [M1] and

[M0], when (3.35) is assumed, will be made in section 3.4. To determine the characteristic exponents, these matrices are inserted in equation (3.27).

3.3 - PERTURBATION METHOD

Another way of solving equations (3.8) is to use a perturbation method. We are going to follow the method described in reference [24].

First we redefine the modal co-ordinates as:

$$\{\delta q_w\} = [B]\{\delta\xi\} \tag{3.36}$$

where $[B]$ is now[6] the modal matrix of

$$[M_b]\{\delta\ddot{q}_w\} + ([Kl_b] + [p_1])\{\delta q_w\} = \{0\}. \tag{3.37}$$

$[B]$ is normalised so that it satisfies the relations

$$[B]^T[M_b][B] = [I] \tag{3.38}$$

$$[B]^T([Kl_b] + [pl])[B] = [\omega_{0j}^2] \tag{3.39}$$

Using the modal co-ordinates and multiplying equations (3.8) by $[B]^T$, we obtain:

$$\{\delta\ddot{\xi}\} + \frac{\beta}{\omega}[B]^T[M_b][B]\{\delta\dot{\xi}\} + [\omega_{0j}^2]\{\delta\xi\} + [B]^T([p_2]\cos(2\omega t) + [p_3]\sin(2\omega t))[B]\{\delta\xi\} = \{0\} \tag{3.40}$$

or

$$\{\delta\ddot{\xi}\} + [\omega_{0j}^2]\{\delta\xi\} + \mu\{\Phi\} = \{0\} \tag{3.41}$$

$$\mu\{\Phi\} = \frac{\beta}{\omega}[B]^T[M_b][B]\{\delta\dot{\xi}\} + [B]^T([p_2]\cos(2\omega t) + [p_3]\sin(2\omega t))[B]\{\delta\xi\}, \tag{3.42}$$

where μ is a small parameter.

---

[6] With this modal matrix, we separate the time dependent coefficients originated by the nonlinear part of the equations of motion from the terms constant in time. The method would work in the same way if the modal matrix was the one defined in (3.15), (3.16), but this formulation is slightly simpler.

Following Floquet's theory, we express the solution of equation (3.41) in the form

$$\{\delta\xi\} = \left\{e^{\lambda_j t}\phi_j\right\} \qquad j=1, \ldots, p_o. \tag{3.43}$$

At $\mu=0$ equation (3.41) has a particular solution of the form

$$\{\delta\xi_0\} = \left\{\delta a_j \cos\left(\nu_j t + \psi_j\right)\right\} \qquad j=1, \ldots, p_o; \tag{3.44}$$

where δa_j and ψ_j are constants which depend on the initial conditions.

We are going to expand $\{\lambda\}$ and $\{\phi\}$ into power series of μ:

$$\{\lambda\} = \{\lambda_0\} + \mu\Delta\{\lambda_1\} + \mu^2\Delta\{\lambda_2\} + \ldots = \{\lambda_0\} + \{\lambda_1\} + \{\lambda_2\} + \ldots \tag{3.45}$$

$$\{\phi\} = \{\phi_0\} + \mu\Delta\{\phi_1\} + \mu^2\Delta\{\phi_2\} + \ldots = \{\phi_0\} + \{\phi_1\} + \{\phi_2\} + \ldots \tag{3.46}$$

where $\{\lambda_0\}$ and $\{\phi_0\}$ represent, respectively, the characteristic exponent and the periodic solution at $\mu=0$ and $\{\lambda_1\}, \{\lambda_2\} \ldots, \{\phi_1\}, \{\phi_2\}, \ldots$ are to be determined.

In order to account for variation of the period of the solution $\{\delta\xi\}$, we also expand its frequency ν_j in a power series of μ:

$$\nu_j = \omega_{oj} + \mu\Delta\omega_{j1} + \mu^2\Delta\omega_{j2} + \ldots \tag{3.47}$$

Insertion of equation (3.47) into equation (3.41) yields

$$\left\{\delta\ddot{\xi}\right\} + \left[\omega_{0j}^2\right]\{\delta\xi\} = -\mu\left\{\Phi\left(\delta\xi_1(0), \ldots, \delta\dot{\xi}_n(0), \omega t\right)\right\} - 2\mu\left[\omega_{0j}^2\right]\left[\Delta\omega_j^{(1)}\right]\{\delta\xi\} + \mu^2\ldots \tag{3.48}$$

The particular solution has the following form

$$\{\delta\xi_j\} = \left\{e^{\sum_{k=0}^{\infty}\mu^k\Delta\lambda_j(k)t}\sum_{k=0}^{\infty}\mu^k\Delta\phi_j(k)\right\}, \tag{3.49}$$

or

$$\{\delta\xi_j\} = \left\{e^{\sum_{k=1}^{\infty}\mu^k\Delta\lambda_j(k)t}\sum_{k=0}^{\infty}\mu^k\varphi_j(k)\right\} = \left\{e^{\sum_{k=1}^{\infty}\lambda_j(k)t}\sum_{k=0}^{\infty}\mu^k\varphi_j(k)\right\}, \tag{3.50}$$

$$j= 1, \ldots, p_o;$$

where

$$\varphi_j(k) = e^{\lambda_0(j)t}\Delta\phi_j(k). \tag{3.51}$$

To apply the classical small parameter technique we insert series (3.50) into equation (3.41) and equate like powers of μ independently to obtain recurrent series of linear equations for $\varphi_j(0), \varphi_j(1), \varphi_j(2)\ldots$. We will make the following approximation:

$$\{\delta\xi_j\} = \left\{e^{\lambda_j(1)t}\left(\varphi_j(0) + \mu\varphi_j(1)\right)\right\} \qquad j=1, \ldots, p_o; \tag{3.52}$$

resulting in

Terms of order μ^0:

$$\{\ddot{\varphi}_j(0)\} + \left[\omega_{0j}^2\right]\{\varphi_j(0)\} = \{0\} \tag{3.53}$$

Terms of order μ^1:

$$\left\{e^{\lambda_j(1)t}\ddot{\varphi}_j(1)\right\} + \left[\omega_{0j}^2\right]\left\{e^{\lambda_j(1)t}\varphi_j(1)\right\} = -\{\Phi\} - 2\left\{\omega_{0j}\Delta\omega_j(1)e^{\lambda_j(1)t}\varphi_j(0)\right\} - 2\left\{\lambda_j(1)e^{\lambda_j(1)t}\dot{\varphi}_j(0)\right\} \tag{3.54}$$

Solution of equation (3.51) yields:

$$\{\varphi_j(0)\} = \left\{\delta a_j \cos\left(\omega_{0j}t + \psi_j\right)\right\} \tag{3.55}$$

where δa_j and ψ_j are constants of integration.

Substituting equation (3.55) into equation (3.52) we obtain

$$\left\{e^{\lambda_j(1)t}\ddot{\varphi}_j(1)\right\} + \left[\omega_{0j}^2\right]\left\{e^{\lambda_j(1)t}\varphi_j(1)\right\} = -\{\Phi\} - 2\left\{\omega_{0j}\Delta\omega_j(1)e^{\lambda_j(1)t}\delta a_j\cos\left(\omega_{0j}t + \psi_j\right)\right\} \tag{3.56}$$
$$+2\left\{\lambda_j(1)e^{\lambda_j(1)t}\omega_{0j}\delta a_j\sin\left(\omega_{0j}t + \psi_j\right)\right\}$$

Making

$$\mu\{\Phi\} = \left([\Lambda 1]\cos(2\omega t) + [\Lambda 2]\sin(2\omega t)\right)\{\delta\xi\} + [\Lambda 3]\{\delta\dot{\xi}\}, \tag{3.57}$$

$$[\Lambda 1] = [B]^T[p2][B], \tag{3.58}$$

$$[\Lambda 2] = [B]^T[p3][B], \tag{3.59}$$

$$[\Lambda 3] = \frac{\beta}{\omega}[B]^T[M_b][B], \tag{3.60}$$

we have

$$\left\{e^{\lambda_j(1)t}\ddot{\varphi}_j(1)\right\}+\left[\omega_{0j}^{\,2}\right]\left\{e^{\lambda_j(1)t}\varphi_j(1)\right\}=-\frac{1}{\mu}\left(\left[\Lambda_1\right]\left\{\frac{1}{2}e^{\lambda_j(1)t}\delta a_j\left(\cos\left(2\omega t+\omega_{0j}t+\psi_j\right)+\cos\left(2\omega t-\omega_{0j}t-\psi_j\right)\right)\right\}+\right.$$
$$\left.\left[\Lambda_2\right]\left\{\frac{1}{2}e^{\lambda_j(1)t}\delta a_j\left(\sin\left(2\omega t+\omega_{0j}t+\psi_j\right)+\sin\left(2\omega t-\omega_{0j}t-\psi_j\right)\right)\right\}-\left[\Lambda_3\right]\left\{e^{\lambda_j(1)t}\delta a_j\omega_{0j}\sin\left(\omega_{0j}t+\psi_j\right)\right\}\right)$$
$$-2\left\{\omega_{0j}\Delta\omega_j(1)e^{\lambda_j(1)t}\delta a_j\cos\left(\omega_{0j}t+\psi_j\right)\right\}+2\left\{\lambda_j(1)\omega_{0j}e^{\lambda_j(1)t}\delta a_j\sin\left(\omega_{0j}t+\psi_j\right)\right\} \tag{3.61}$$

Vanishing of secular terms (unbounded terms) must be ensured. These exist if the harmonics on the right hand side of equation (3.61) provide terms with frequency ω_{0j}. The following cases will be discussed:

1 - Nonresonant case

$\omega\neq\omega_{0j}$ and $\left|\omega_{0k}\pm\omega_{0j}\right|\neq 2\omega$ at all values j, k = 1, ..., p_o.

2 - Simple resonant case

$\omega=\omega_{0j}$ for some j between 1 and p_o.

Nonresonant Case

In this case the mixed harmonic terms with frequencies $2\omega\pm\omega_{0j}$ in equations (3.61) do not give rise to harmonic components of frequency ω_{0j}. Therefore, the conditions which ensure vanishing of $\cos(\omega_{0j}t)$ and $\sin(\omega_{0j}t)$ terms on the right hand side these equations are simply as follows:

$$\frac{1}{\mu}\Lambda_3(j,j)\sin\left(\psi_j\right)-2\Delta\omega_j(1)\cos\left(\psi_j\right)+2\lambda_j(1)\sin\left(\psi_j\right)=0 \tag{3.62}$$

$$\frac{1}{\mu}\Lambda_3(j,j)\cos\left(\psi_j\right)+2\Delta\omega_j(1)\sin\left(\psi_j\right)+2\lambda_j(1)\cos\left(\psi_j\right)=0 \tag{3.63}$$

and hence the required correction coefficients $\left\{\lambda_j(1)\right\}$ are

$$\lambda_j(1)=-\frac{1}{\mu}\frac{\Lambda_3(j,j)}{2}\pm i\Delta\omega_j(1). \tag{3.64}$$

It follows that our solution (3.52) in the first approximation is defined as:

$$\delta\xi_j = e^{\left(-\frac{1}{\mu}\frac{\Lambda_3(j,j)}{2}\pm i\Delta\omega_j(1)\right)t}\varphi_j(0) \tag{3.65}$$

and after insertion of equation (3.55), its real part is reduced to

$$\delta\xi_j = \delta a_j e^{\left(-\frac{1}{\mu}\frac{\Lambda_3(j,j)}{2}\right)t}\cos\left(\omega_{0j}t+\psi_j\right)\cos\left(\Delta\omega_j(1)t\right). \tag{3.66}$$

We conclude that in dissipative systems, in which $\Lambda_3(j,j)>0$, j=1, ..., p_o, all co-ordinates $\delta\xi_j$ tend to zero; consequently, the system is stable in nonresonant regions.

Simple Resonance

If $\omega=\omega_{0s}$ for a certain s, the mixed harmonic terms on the right hand side of equations (3.54) provide a harmonic component with frequency ω_{0s} ($2\omega-\omega_{0s}=\omega_{0s}$). This may originate secular terms in the function $\varphi_s(1)$ and hence also in the co-ordinate $\delta\xi_s$. Note that all other co-ordinates are not endangered as conditions (3.66) remain valid for them.

The condition of vanishing secular terms now is stated as:

$$\begin{aligned}&\frac{1}{\mu}\left(-\frac{1}{2}\Lambda_1(s,s)\delta a_s\cos(\omega_{0s}t-\psi_s)-\frac{1}{2}\Lambda_2(s,s)\delta a_s\sin(\omega_{0s}t-\psi_s)+\Lambda_3(s,s)\delta a_s\omega_{0s}\sin(\omega_{0s}t+\psi_s)\right)\\&-2\omega_{0s}\Delta\omega_s(1)\delta a_s\cos(\omega_{0s}t+\psi_s)+2\lambda_s(1)\delta a_s\omega_{0s}\sin(\omega_{0s}t+\psi_s)=0\end{aligned} \tag{3.67}$$

Terms in cos($\omega_{0s}t$)

$$\begin{aligned}&\frac{1}{\mu}\left(-\frac{1}{2}\Lambda_1(s,s)\cos(\psi_s)+\frac{1}{2}\Lambda_2(s,s)\sin(\psi_s)+\Lambda_3(s,s)\omega_{0s}\sin(\psi_s)\right)\\&-2\omega_{0s}\Delta\omega_s(1)\cos(\psi_s)+2\lambda_s(1)\omega_{0s}\sin(\psi_s)=0\end{aligned} \tag{3.68}$$

Terms in sin($\omega_{0s}t$)

$$\begin{aligned}&\frac{1}{\mu}\left(-\frac{1}{2}\Lambda_1(s,s)\sin(\psi_s)-\frac{1}{2}\Lambda_2(s,s)\cos(\psi_s)+\Lambda_3(s,s)\omega_{0s}\cos(\psi_s)\right)\\&+2\omega_{0s}\Delta\omega_s(1)\sin(\psi_s)+2\lambda_s(1)\omega_{0s}\cos(\psi_s)=0\end{aligned} \tag{3.69}$$

Therefore, we conclude that

$$\lambda_s(1)=\left(-\frac{\Lambda_3(s,s)}{2\mu}+\frac{1}{4\omega_{0s}}\sqrt{\frac{\Lambda_1^2(s,s)}{\mu^2}+\frac{\Lambda_2^2(s,s)}{\mu^2}-16\omega_{0s}^2\Delta\omega_s^2(1)}\right) \tag{3.70}$$

or

$$\lambda_s(1)=\left(-\frac{\Lambda_3(s,s)}{2\mu}-\frac{1}{4\omega_{0s}}\sqrt{\frac{\Lambda_1^2(s,s)}{\mu^2}+\frac{\Lambda_2^2(s,s)}{\mu^2}-16\omega_{0s}^2\Delta\omega_s^2(1)}\right) \tag{3.71}$$

If $\lambda_s(1)$ is defined by equation (3.71), then it has always a negative real part. If, on the other hand, it is defined by equation (3.70), its real part vanishes if:

$$\Delta\omega_s^2(1)=\frac{1}{16\omega_{0s}^2\mu^2}\left(\Lambda_1^2(s,s)+\Lambda_2^2(s,s)-4\omega_{0s}^2\Lambda_3^2(s,s)\right) \tag{3.72}$$

and is positive if

$$-\frac{1}{4\mu\omega_{0s}}\sqrt{\Lambda_1^2(s,s)+\Lambda_2^2(s,s)-4\omega_{0s}^2\Lambda_3^2(s,s)}<\Delta\omega_s(1)<\frac{1}{4\mu\omega_{0s}}\sqrt{\Lambda_1^2(s,s)+\Lambda_2^2(s,s)-4\omega_{0s}^2\Lambda_3^2(s,s)} \tag{3.73}$$

The former condition (3.72), corresponds to the stability limit; the latter, equation (3.73), defines the simple unstable region where the coordinate $\delta\xi_s$ grows exponentially over time.

Finally, the region of frequency, ω, where the simple instability occurs is defined by

$$\omega_{0s}-\frac{1}{4\omega_{0s}}\sqrt{\Lambda_1^2(s,s)+\Lambda_2^2(s,s)-4\omega_{0s}^2\Lambda_3^2(s,s)}<\omega<\frac{1}{4\omega_{0s}}\sqrt{\Lambda_1^2(s,s)+\Lambda_2^2(s,s)-4\omega_{0s}^2\Lambda_3^2(s,s)}+\omega_{0s} \tag{3.74}$$

3.4 - DETERMINANT OF THE JACOBIAN OF {*F*}

For one degree of freedom systems it has been proved that solutions after (before) and in the vicinity of the backbone curve, with a positive (negative) slope are unstable [9, 24].

Lewandowski [34] presented, for multi-degree of freedom undamped systems, a proof that the sign of the determinant of the Jacobian of $\{F\}$ is zero in the stability limit. We are going to follow his idea and, taking advantage of the transformation (3.18), generalise it to proportionally damped systems.

We want to study the evolution with time of solutions to the variational equation (3.20), which is re-written here:

$$\left\{\delta\ddot{\bar{\xi}}\right\}+\left(\left[\omega_{0j}^2\right]-\frac{1}{4}\left(\frac{\beta}{\omega}\right)^2[I]+[B]^T\left([p_1]+[p_2]\cos(2\omega t)+[p_3]\sin(2\omega t)\right)[B]\right)\left\{\delta\bar{\xi}\right\}=\{0\} \quad (3.20)$$

Now, following Hayashi [9, pag. 93], we will express the solution of (3.20) in the form:

$$\left\{\delta\bar{\xi}\right\}=e^{\lambda t}\left(\{b_1\}\cos(\omega t)+\{a_1\}\sin(\omega t)\right) \quad (3.35)$$

which should allow us to determine, in a first approximation, the first order simple unstable region.

Inserting (3.35) into (3.20) and applying the HB method, we find

terms in cos(ωt)

$$\left(\left[\omega_{0j}^2\right]+\left(\lambda^2-\omega^2-\frac{1}{4}\left(\frac{\beta}{\omega}\right)^2\right)[I]+[B]^T\left([p_1]+\frac{1}{2}[p_2]\right)[B]\right)\{b_1\}+\left(2\lambda\omega+\frac{1}{2}[B]^T[p_3][B]\right)\{a_1\}=\{0\} \quad (3.75)$$

terms in sin(ωt)

$$\left(\frac{1}{2}[B]^T[p_3][B]-2\lambda\omega\right)\{b_1\}+\left(\left[\omega_{0j}^2\right]+\left(\lambda^2-\omega^2-\frac{1}{4}\left(\frac{\beta}{\omega}\right)^2\right)[I]+[B]^T\left([p_1]-\frac{1}{2}[p_2]\right)[B]\right)\{a_1\}=\{0\} \quad (3.76)$$

The nonlinear stiffness matrix is defined as

$$[Knl]=[K4]-2[K2]^T\left[K1_p\right]^{-1}[K2] \quad (3.77)$$

The cosine and sine coefficients of $[Knl]\{q_w\}$ are obtained by the harmonic balance method and, for $\{q_w\}$ defined in (3.1), have the following form:

$$\{F_1\}=\frac{2}{T}\int_0^T[Knl]\{q_w\}\cos(\omega t)\,dt=\left(\frac{3}{4}KNL1+\frac{1}{4}KNL3\right)\{w_c\}+\frac{1}{4}KNL2\{w_s\} \quad (3.78)$$

$$\{F_2\}=\frac{2}{T}\int_0^T[Knl]\{q_w\}\sin(\omega t)\,dt=\frac{1}{4}KNL2\{w_c\}+\left(\frac{1}{4}KNL1+\frac{3}{4}KNL3\right)\{w_s\} \tag{3.79}$$

Applying the derivation rule for composite functions we obtain the derivatives of $\{F_1\}$ and $\{F_2\}$:

$$[D_{11}]=\frac{\partial\{F_1\}}{\partial\{w_c\}}=\frac{2}{T}\int_0^T\frac{\partial}{\partial\{q_w\}}\left([Knl]\{q_w\}\right)\frac{\partial\{q_w\}}{\partial\{w_c\}}\cos(\omega t)\,dt \tag{3.80}$$

$$[D_{12}]=\frac{\partial\{F_1\}}{\partial\{w_s\}}=\frac{2}{T}\int_0^T\frac{\partial}{\partial\{q_w\}}\left([Knl]\{q_w\}\right)\frac{\partial\{q_w\}}{\partial\{w_s\}}\cos(\omega t)\,dt \tag{3.81}$$

$$[D_{21}]=\frac{\partial\{F_2\}}{\partial\{w_c\}}=\frac{2}{T}\int_0^T\frac{\partial}{\partial\{q_w\}}\left([Knl]\{q_w\}\right)\frac{\partial\{q_w\}}{\partial\{w_c\}}\sin(\omega t)\,dt \tag{3.82}$$

$$[D_{22}]=\frac{\partial\{F_2\}}{\partial\{w_s\}}=\frac{2}{T}\int_0^T\frac{\partial}{\partial\{q_w\}}\left([Knl]\{q_w\}\right)\frac{\partial\{q_w\}}{\partial\{w_s\}}\sin(\omega t)\,dt \tag{3.83}$$

[p1], [p2] and [p3] were derived using the HBM; they are Fourier expansions of the Jacobian of $[Knl]\{q_w\}$. Let us re-write [p1], [p2] and [p3] as:

$$[p_1]=\frac{1}{T}\int_0^T\frac{\partial}{\partial\{q_w\}}\left([Knl]\{q_w\}\right)dt=\frac{2}{T}\int_0^T\frac{\partial}{\partial\{q_w\}}\left([Knl]\{q_w\}\right)\cos^2(\omega t)\,dt-$$

$$\frac{1}{T}\int_0^T\frac{\partial}{\partial\{q_w\}}\left([Knl]\{q_w\}\right)\cos(2\omega t)\,dt=\frac{2}{T}\int_0^T\frac{\partial}{\partial\{q_w\}}\left([Knl]\{q_w\}\right)\frac{\partial\{q_w\}}{\partial\{w_c\}}\cos(\omega t)\,dt-\frac{1}{2}[p_2]$$

$$=\frac{\partial F_1}{\partial\{w_c\}}-\frac{1}{2}[p_2]=[D_{11}]-\frac{1}{2}[p_2] \tag{3.84}$$

$$[p_2]=\frac{2}{T}\int_0^T\frac{\partial}{\partial\{q_w\}}\left([Knl]\{q_w\}\right)\cos(2\omega t)dt=\frac{2}{T}\int_0^T\frac{\partial}{\partial\{q_w\}}\left([Knl]\{q_w\}\right)\left(\cos^2(\omega t)-\sin^2(\omega t)\right)dt$$

$$=2[p_1]-\frac{4}{T}\int_0^T\frac{\partial}{\partial\{q_w\}}\left([Knl]\{q_w\}\right)\frac{\partial\{q_w\}}{\partial\{w_s\}}\sin(\omega t)\,dt=2[p_1]-2\frac{\partial\{F_2\}}{\partial\{w_s\}}=2[p_1]-2[D_{22}] \tag{3.85}$$

$$[p_3]=\frac{2}{T}\int_0^T \frac{\partial}{\partial\{q_w\}}\left([Knl]\{q_w\}\right)\sin(2\omega t)dt=\frac{4}{T}\int_0^T \frac{\partial}{\partial\{q_w\}}\left([Knl]\{q_w\}\right)\frac{\partial\{q_w\}}{\partial\{w_c\}}\sin(\omega t)\,dt=$$

$$2\frac{\partial\{F_2\}}{\partial\{w_c\}}=2[D_{21}] \tag{3.86}$$

$$[p_3]=\frac{4}{T}\int_0^T \frac{\partial}{\partial\{q_w\}}\left([Knl]\{q_w\}\right)\frac{\partial\{q_w\}}{\partial\{w_s\}}\cos(\omega t)\,dt=2\frac{\partial\{F_1\}}{\partial\{w_s\}}=2[D_{12}] \tag{3.87}$$

Above, we took into consideration that

$$\frac{\partial\{q_w\}}{\partial\{w_c\}}=[I]\cos(\omega t) \tag{3.88}$$

$$\frac{\partial\{q_w\}}{\partial\{w_s\}}=[I]\sin(\omega t) \tag{3.89}$$

Writing equations (3.75) and (3.76) in matrix form, we have:

$$\left(\lambda^2[I]+\lambda[M_1]+[M_0]\right)\begin{Bmatrix}b_1\\a_1\end{Bmatrix}=\begin{Bmatrix}0\\0\end{Bmatrix} \tag{3.90}$$

where

$$[M_1]=\begin{bmatrix}0 & 2\omega[I]\\ -2\omega[I] & 0\end{bmatrix} \tag{3.91}$$

$$[M_0]=\begin{bmatrix}[B]^T[D_{11}][B]-\left(\omega^2+\left(\frac{1}{2}\frac{\beta}{\omega}\right)^2\right)[I]+[\omega_{0j}{}^2] & [B]^T[D_{12}][B]\\ [B]^T[D_{21}][B] & [B]^T[D_{22}][B]-\left(\omega^2+\left(\frac{1}{2}\frac{\beta}{\omega}\right)^2\right)[I]+[\omega_{0j}{}^2]\end{bmatrix} \tag{3.92}$$

Equation (3.90) can be transformed into an eigenvalue problem with the form (3.27) and the characteristic exponents can be determined in that way.

Now, we are going to expand Lewandowski's [34] idea to systems with mass proportional damping.

The eigenvalue problem resulting from (3.90) is called conservative gyroscopic, because matrices [I] and $[M_0]$ are symmetric and matrix $[M_1]$ is skew-symmetric [35]. Its eigenvalues are purely imaginary or purely real [34]. For imaginary λ

$$\mathrm{Re}\left(\lambda - \frac{1}{2}\frac{\beta}{\omega}\right) = -\frac{1}{2}\frac{\beta}{\omega} \tag{3.93}$$

and for real λ

$$\mathrm{Re}\left(\lambda - \frac{1}{2}\frac{\beta}{\omega}\right) = \lambda - \frac{1}{2}\frac{\beta}{\omega}. \tag{3.94}$$

If λ is imaginary the solution is always stable; if λ is real the stability limit is defined by

$$\mathrm{Re}\left(\lambda - \frac{1}{2}\frac{\beta}{\omega}\right) = 0 \Leftrightarrow \lambda = \frac{1}{2}\frac{\beta}{\omega}. \tag{3.95}$$

Inserting (3.95) in (3.90) we arrive at

$$\begin{bmatrix} [B]^T[D_{11}][B] - \omega^2[I] + [\omega_{0j}{}^2] & [B]^T[D_{12}][B] + \beta \\ [B]^T[D_{21}][B] - \beta & [B]^T[D_{22}][B] - \omega^2[I] + [\omega_{0j}{}^2] \end{bmatrix} \begin{Bmatrix} b_1 \\ a_1 \end{Bmatrix} = \begin{Bmatrix} 0 \\ 0 \end{Bmatrix} \tag{3.96}$$

The matrix in the previous equation is $[B]^T[D][B]$, where [D] is the Jacobian of $\{F\}$ given by

$$[D] = \frac{\partial}{\partial\{q_w\}}\{F\} \tag{3.97}$$

A non-trivial solution of (3.96) exists if

$$\det\left([B]^T[D][B]\right) = 0 \Leftrightarrow |B|^2|D| = 0 \Leftrightarrow |D| = 0, \tag{3.98}$$

The last equivalence is true because [B] is a non-singular matrix, since the modal vectors are linearly independent; because the determinant of the product of matrices is equal to the product of the determinants and because the determinant of the tranpose matrix is equal to the determinant of the original matrix. Thus, we proved that in the stability limit, the determinant of the Jacobian of $\{F\}$, $|D|$, is zero.

$|D|$ is a polynomial in the coefficients $\{w_c\}$ and $\{w_s\}$ and in ω; therefore, it is a continuous function in those coefficients. All the experimental and numerical analysis of nonlinear vibration of beams, indicate that the shape of vibration, defined in our model by $\{w_c\}$ and $\{w_s\}$, is a continuous function of the amplitude and the frequency of vibration. Thus, we conclude that $|D|$ varies in a continuous way through the FRF

curve. Hence, if there is a change in its sign between two consecutive points of the FRF curve, then $|D|=0$ for a particular point between these two. In that particular point, the stability limit may have been crossed.

Therefore, in order to execute the first order study of the simple stability of the solutions, we only have to determine the characteristic exponents of one solution and, thereafter, when |D| changes sign or when |D| is approximately zero. As |D| is needed in the continuation method and, when the Newton method is applied, can be easily calculated from [D], this results in substantial time savings. All numerical results in this report indicate that $|D|>0$ in stable regions and $|D|<0$ in unstable regions; however, this was not proved.

4 - APPLICATIONS

4.1 - INTRODUCTION

In this section, we are going to analyse the response of a beam clamped at both ends, excited by a point harmonic force applied in the middle of the beam, by a plane harmonic wave and by a harmonic wave at grazing incidence. All the forces are applied in the transverse direction.

Since the beam and the boundary conditions have symmetric properties, when the force is applied in the middle of the beam and when the force is exerted by a harmonic plane wave at normal incidence, only symmetric out of-plane shape functions and antisymmetric in-plane shape functions need to be used[7]. For a wave at grazing incidence symmetric and anti-symmetric shape functions must be used.

Using the point harmonic force, the convergence of the HFEM solution with the number of shape functions, the influence of in-plane displacements and the stability of the solutions will be studied. Also with the point harmonic force, the frequency

[7] To check if the nonlinearity introduced any coupling and consequent antisymmetric terms in the response, a model including symmetric and antisymmetric, in- and out-of-plane shape functions was considered. It was confirmed that, with these boundary conditions and with the one harmonic representation of the solution's time dependency, there is no such coupling.

response curve for a beam analysed in reference [30], will be derived and compared with the experimental one. Finally, the response to a harmonic plane wave and to a plane wave at grazing incidence will be investigated.

The beam under analysis was made of aluminium alloy with the reference 7075-T6, which has the following properties [13]:

$E = 7.172*10^{10}$ N/m^2, $\rho = 2800$ kg/m^3, $\upsilon = 0.33$.

The geometric properties of this beam are as follows:

h=0.002 m, b=0.02 m, L = 0.405 m [8], $A=4\times10^{-5}$ m^2,

$I=\frac{1}{12}bh^3 = 1.333(3)\times10^{-11}$ m^4, $r=\sqrt{\frac{I}{A}}=5.7735\times10^{-4}$ m.

For aluminium the loss factor assumes values typically in the range 0.0001-0.01. Regarding the loss factor of the first mode, from reference [30], pag.32, we take the value 0.01 (ζ=0.5%) as the most typical. However, the measured value was approximately equal to 0.038 ($\zeta\cong$1.9%). These values are for the loss factor, α, present in the equation of motion, which, when a one mode approximation is used and only linear terms are considered, takes the form:

$$\ddot{x}+\alpha\omega_0\dot{x}+{\omega_0}^2x=\ddot{x}+2\varsigma\omega_0\dot{x}+{\omega_0}^2x=\frac{F}{m}\cos(\omega t) \qquad (4.1)$$

When applying the HFEM, considering modal co-ordinates, we have

$$\{\ddot{\xi}\}+\frac{\beta}{\omega}[I]\{\dot{\xi}\}+[{\omega_{0j}}^2]\{\xi\}=[B]^T\{\bar{F}\}. \qquad (4.2)$$

Equalising the damping coefficient of equation (4.2) for the first mode and at the first natural frequency to $\alpha\omega_0$ we have

$$\beta={\omega_{01}}^2\times\alpha. \qquad (4.3)$$

It should be noted that Wolfe did not think that the measured damping ratio was only due to material damping. He also attributed the obtained value to damping in the joints and to the coil magnet arrangement used to excite the beam.

[8] Except in the comparison with experimental results, where L=0.406 (value of Wolfe's clamped-clamped beam length).

4.2 - HARMONIC POINT EXCITATION

4.2.1 - Study of convergence with number of shape functions

We can see in Table 1 that with four out-of-plane and four in-plane shape functions, convergence of the value of the first linear natural frequency is achieved. This number of shape functions will be the starting value for our analysis.

Table 1 - Natural linear frequencies of the cc beam (rad/s). Mode 1.

Exact [8]	p_o=2, p_i=2	p_o=3, p_i=3	p_o=4, p=4$_i$	p_o=5, p_i=5
396.6	396.613 239	396. 605 011	396. 605 008	396. 605 008

In Figures 1, 2 and 3 we can see the FRFs in the vicinity of the first, third and fifth mode, obtained when a force P of 0.03 N was applied. Near the first mode there is no increase in accuracy by using more than four out-of-plane and four in-plane shape functions (p_o=4, p_i=4). However, for the third mode, as the amplitude of vibration grows, the results obtained with p_o=4 and p_i=4 depart from the ones obtained with more shape functions. The FRF curve constructed with p_o=5 and p_i=5 is quite similar to the coincident FRFs obtained with p_o=6 and p_i=6 and p_o=7 and p_i=7. In the neighbourhood of the fifth mode, convergence seems to be achieved with p_o=8 and p_i=8.

4.2.2 - Influence of in-plane displacements

In Figure 4 the FRFs obtained considering and neglecting the in-plane displacements are compared. As in references [1] and [15], we found that the in-plane displacements 'reduce' the non-linearity, in the sense that the non-linearity caused by them is of the soft spring type as opposed to the hard spring type non-linearity caused by the transverse displacements. This 'reduction' of nonlinearity happens in-spite of the negligence of in-plane inertia. It is due, as the formulation of the nonlinear stiffness matrix (2.14) shows, to the effects of in-plane deformation on the stiffness of the structure.

4.2.3 - Study of stability

In this section, we present and compare the results obtained with different methods of studying the stability of the solutions. These methods were introduced in section 3. In all cases p_o=6 and p_i=6 and the excitation force was a point harmonic force with P = 0.03 N.

After the resonance frequency and in its neighbourhood, when the slope of the curve is positive, we would expect the solutions to be unstable. As we can see, the stability study carried out with the perturbation method, Figure 5, resulted in the definition of some points in those conditions as stable. Using the HBM, with (3.21), the stability properties of the solutions are well determined except for a point very near to the maximum amplitude of vibration (Figures 6 and 7). This point is better detected in the phase plot, Figure 7. The introduction of more harmonics in (3.21) , k=3 was tried, did not change the stability results. Using the HBM, but with solution (3.35), the stability of the solutions corresponds to what was expected (Figure 8).

In Figures 9 and 10, the FRF around the third resonance frequency is shown, with the stability study carried out using the HBM, equation (3.21), with k=1 and k=3, respectively. We see that some points after the resonance frequency and with a positive slope, were determined as stable. There is no visible improvement from the k=1 to the k=3 cases. The results of a similar study, but using solution (3.35), were correct as it is shown in Figure 11.

The stability results obtained using $|D|$, as explained in section 3.4, were similar to the ones using the harmonic balance method with solution (3.35). The method based on |D| is highly convenient and will be used to determine the stability of the solutions in all the cases of the following sections.

4.2.4 - Comparison with experimental results

In Figures 12 and 13 we can see the comparison between the FRF obtained with the HFEM, using p_o=6 and p_i=6 shape functions, and the experimental results [30]

when a force P = 0.134 N is applied in the centre of the beam. Two values were used for the loss factor: α=0.01 and α=0.038.

The HFEM provides a FRF with a slope similar to the experimental one around the resonance frequency. This indicates that the nonlinear stiffness is well approximated by the model.

The turning point corresponding to the largest amplitude of vibration, where the jump phenomena occurs, obtained with the HFEM, point **A**, does not match the experimental one, point **B**. With the typical value used for the loss factor in aluminium alloys, 0.01, the maximum amplitude of vibration was more than double of the one measured. However, the HFEM solutions represented in Figure 12 after point **B** are very close. Thus, in a real system, a small perturbation would easily make the shape of vibration change into an unstable one and a change, or jump, to another stable shape of vibration could be observed before the largest theoretical amplitude of vibration was achieved. With the measured loss factor, 0.038, the largest amplitude of vibration of the HFEM results, was around a half of the measured maximum amplitude. It is thus confirmed, that the damping coefficient is of paramount importance in the determination of the maximum amplitude of vibration of nonlinear systems.

Wolfe [30] attributed the measured damping to more than simple material damping. We would say that, for engineering purposes, where the maximum amplitude of vibration is of importance in order to determine the efforts to which the structure is subjected, the consideration of the material damping alone in the HFEM model provides a result on the safe side.

4.3 - RESPONSE TO A NORMALLY INCIDENT HARMONIC PLANE WAVE

If an acoustic harmonic plane wave impinges on the beam surface in the normal direction, the force exerted per unit displacement is given by

$$\overline{P}_d(x,t) = bP\cos(\omega t) \qquad (4.4)$$

where P is the magnitude of the pressure and ω is the frequency of the harmonic wave.

Figures 14 and 15 depict the FRFs in the vicinity of the first and third modes, obtained when a harmonic plane wave with an amplitude P = 5 N/m^2 was applied. Due to the symmetric form of the external force applied, the second mode is not excited.

4.4 - RESPONSE TO A HARMONIC PLANE WAVE AT GRAZING INCIDENCE

When the excitation considered is a grazing acoustic harmonic wave travelling in the direction of the axis of the beam, the force per unit displacement at an arbitrary point is given by

$$\overline{P}_d(x,t) = bP\cos(\omega t - kx),\ k = \frac{\omega}{c}, \tag{4.5}$$

where P is the pressure amplitude, k is the wave number and c is the speed of sound in air. In this case the vector of generalised forces of equation (2.18) is

$$\{F\} = \begin{Bmatrix} b\int_L P\cos(kx)\{N^w(x)\}dL \\ b\int_L P\sin(kx)\{N^w(x)\}dL \end{Bmatrix} \tag{4.6}$$

The quite complex expressions for the vector of generalised forces were generated using Maple. They were very affected by numerical round-off errors; therefore it was necessary to use a large number of digits to derive them.

Because a wave at grazing incidence, travelling along the longitudinal axis of the beam, is asymmetric, both symmetric and antisymmetric modes are excited. In Figures 16, 17 and 18 the FRFs in the vicinity of the first, second and third modes, obtained when an excitation at P of 5 N/m^2 was applied are shown. The largest amplitudes of vibration decrease as we go from the first to the third modes.

5 - CONCLUSIONS

In this work, the steady state response of beams vibrating with geometrically nonlinearity has been studied. For that we used the hierarchical finite element method, a continuation method and symbolic manipulation.

It was shown that with the HFEM good approximation to the solution are obtained using only a few degrees of freedom. The embedding properties[9] of the HFEM and the easy way in which the number of degrees of freedom of the HFEM model are reduced, benefiting from the symmetry properties of the problem, allow significant time savings. The relatively small number of degrees of freedom of the HFEM model, also reduces the implications of the inclusion of damping in the model, which doubles that number.

For the amplitudes of vibration considered (less than the thickness of the beam), the FRF up to the fifth mode was accurately described with six out-of-plane shape functions and six in-plane shape functions, in a total of twelve degrees of freedom for the model with damping. The fifth mode required the use of more shape functions. If modes of order higher than fifth are to be studied, then the inclusion of more elements instead more shape functions should be considered. If shape functions of an excessive high order are used, the construction of the nonlinear matrices involved in the HFEM model becomes quite lengthy. The versatility of including either more shape functions or more elements is an advantage of a general version of the finite element method, which is called *h-p* version [32].

When the nonlinearity becomes larger due to larger amplitudes of vibration, convergence with the Newton-Raphson method is difficult to achieve. For regions with more than one solution, an automatic description of the frequency response curve and determination of turning points using the Newton-Raphson method is not easy. With the continuation method the FRF curves were completely described and the turning points were determined.

The comparison with experimental results showed a very good prediction of the slope of the FRF around the first mode. The largest amplitude of vibration and the correspondent turning and jump point, are influenced greatly by the amount of

[9] Here we include the advantages in the derivation of the nonlinear stiffness matrix.

damping considered. If the damping coefficient is increased the largest amplitude of vibration will be smaller and, consequently, so will be the geometrical nonlinearity.

The effect of the in-plane displacements was investigated, by using the flexibility of choosing the shape functions in the HFEM model. It was shown that they cause a soft-type nonlinearity.

In the stability study, the perturbation method is quicker than the harmonic balance method. However, the perturbation method is limited to small nonlinearities. When using the HBM, expression (3.21) gave wrong results for points very close to the backbone curve[10], at large amplitudes of vibration. This happened, regardless of the consideration of more harmonics to express the time dependence of the solution of the variational equations (3.20). The equations of motion (2.17), from which we obtained the solutions, result from an approximate method, since higher order harmonics were neglected. In our case study, the nonlinearity is quite important and the stable and unstable solutions are very close for the larger amplitudes of vibration; therefore, any small imprecision can give rise to wrong results in the study of the stability. A similar problem was detected in [7] for single degree of freedom systems. However, the consideration of expansion (3.35), which is of the same kind as the one used to solve the equations of motion, leads to an accurate stability study.

To determine the characteristic exponents that establish the stability of the solution, we solve an eigenvalue problem. Due to the reduced number of degrees of freedom of the HFEM model this is quickly solved. More important, it was proven that $|D|$ is equal to zero in the stability limit. Thus, we only have to determine the characteristic exponents of the first solution and when there is an indication that $|D|$ was zero for a particular point, to check if the stability of the solution changed. This results in significant time savings.

Symbolic manipulation allowed an exact derivation of the matrices involved in the HFEM model, an exact derivation of Jacobian matrix necessary in the continuation and Newton methods, and was helpful in the separation of the coefficients of each harmonic when applying the HBM.

[10] Curve that relates the amplitude with the 'natural frequency' of vibration.

ACKNOWLEDGEMENT

P. Ribeiro acknowledges the support of PRAXIS XXI, *JNICT*, Portugal.

REFERENCES

[1] - Atluri, S.; 'Nonlinear vibrations of a hinged beam including nonlinear effects'; Transactions of the ASME Journal of Applied Mechanics, 40, 1973, 121-126.

[2] - Bennet, J. A. And Eisley, 'A multiple-degree-of freedom approach to nonlinear beam vibrations'; Journal of the American Institute of Aeronautics and astronautics, 8, 1970, 734-739.

[3] - Bolotin, V. V.; *The Dynamic Stability of Elastic Systems*; Holden Day, Inc.; 1964.

[4] - Caughey, T. K.; 'Classical normal modes in damped linear dynamic systems'; Transactions of the ASME, Journal of Applied Mechanics; 27, 1960, 269-271.

[5] - Cheung, Y. K. And Lau, S. L.; 'Incremental time-space finite strip method for non-linear structural vibrations'; Earthquake Engng. and Structural Dynamics, 10, 1982, 239-253.

[6] - Han, W; *The Analysis of isotropic and laminated rectangular plates including geometrical non-linearity using the p-version finite element method*; PhD Thesis, University of Southampton, 1993.

[7] - Hamdan, M.N.; Burton, T.D.; 'On the steady state response and stability of non-linear oscillators using harmonic balance'; Journal of Sound and Vibration, 166(2), 1993, 255-266.

[8]- Harris, Cyril M.; ed. *Shock and Vibration Handbook*; Third edition, Mc Graw-Hill, 1988.

[9] - Hayashi, C; *Nonlinear Oscillations in Physical Systems*; Princeton University Press; 1985 or McGraw-Hill, Inc. 1964.

[10] - Hsu, C S; 'On the parametric excitation of a dynamic system having multiple degrees of freedom'; Transactions of the ASME, Journal of Applied Mechanics, 30, 1963, 367-372.

[11] - Leung, A.Y.T. and Fung, T.C.; 'Non-linear steady state vibration of frames by finite element method'; International Journal for Numerical Methods in Engineering, 28, 1989, 1599-1618.

[12] - Lewandowski, R.; 'Non-linear free vibrations of beams by the finite element and continuation methods'; Journal of Sound and Vibration, 170(5), 1994, 577-593.

[13] - Lyman, Taylor, edited by; *Properties and Selection of Metals*, Metals Handbook, Vol. 1, 8th edition; American Society for Metals; 1961.

[14] - Ma, Ai-Jun; Chen, Su-Huan; Song, Da-Tong; A new method of nonlinear analysis for large deflection forced vibration of beams; Finite Elements in Analysis and Design, 20, 1995, 39-46

[15] - Mei, C and Decha-Umphai; 'A finite element method for non-linear forced vibrations of beams'; Journal of Sound and Vibration, 102, 1985, 369-380.

[16] - Meirovitch, L.; *Elements of Vibration Analysis*; McGraw-Hill, 1986.

[17] - Mentel, T. J.; 'Vibrational energy dissipation at structural support junctions'; Colloquium on Structural Damping; edited by E J Ruzicka; 1959, 89-116.

[18] - Nayfeh, A. H.; Mook, D.T.; *Nonlinear Oscillations*; John Wiley & Sons, New York, 1979.

[19] - Petyt, M; *Introduction to Finite Element Vibration Analysis*; Cambridge University Press, 1990.

[20] - Ribeiro, P.; Petyt, M.; *Study of nonlinear free vibration of beams by the hierarchical finite element method*; ISVR Technical Memorandum No.773; November 1995.

[21] - Rayleigh; *The Theory of Sound*, vol. 1; Dover, New York, pp. 130, 1877.

[22] - Redfern, Darren; *The Maple Handbook*; Springer-Verlag, 1994.

[23]- Seidel, Rüdiger; *From Equilibrium to Chaos. Pratical Bifurcation and Stability Analysis*; Elsevier Science Publishing Co., Inc.,1988.

[24] - Szempliń'ska-Stupnicka, W.; *The Behaviour of Non-linear Vibrating Systems*; Kluwer Academic Publishers, 1990.

[25] - Szempliń'ska-Stupnicka, W; 'The generalised harmonic balance method for determining the combination resonance in the parametric dynamic systems'; Journal of Sound and Vibration, 58, 1978, 347-361.

[26] - Takahashi, K.; 'A method of stability analysis for non-linear vibration of beams'; Journal of Sound and Vibration, 67(8), 1979, 43-54.

[27] - Takahashi, K.; 'Instability of parametric systems with non-uniform damping'; Journal of Sound and Vibration, 85(2), 1982, 257-262.

[28] - Tseng, W. Y.; Dugundji; 'Nonlinear vibrations of a beam under harmonic excitation'; Transactions of the ASME, Journal of Applied Mechanics, 37, 1970; 292-297.

[29] - Wang, S. S.; Huseyn, K.; 'Bifurcations and stability properties of nonlinear systems with symbolic software'; Mathematical Comput. Modelling, 18 (8), 1993, 21-38.

[30] - Wolfe, Howard; *An experimental investigation of nonlinear behaviour of beams and plates excited to high levels of dynamic response*; Ph.D. Thesis, University of Southampton, 1995.

[31] - Federkov, G. V.; 'On the damping of the free vibrations of systems with many degrees of freedom'; Tr. Mosk. Inst. Inzh. Transp., 76, 1952, 135-140.

[32] - Szabo', Barna; Babuska, Ivo; *Finite Element Analysis*; John Wiley & Sons, Inc., New York, 1991.

[33] - Meirovitch, L.; Baruh, H.; 'On the inclusion principle for the hierarchical finite element method'; International Journal for Numerical Methods in Engineering, 19, 1983, 281-291.

[34] - Lewandowski, R.; 'Non-linear, steady-state analysis of multispan beams by the finite element method'; Computers and Structures, 39, 1991, 83-93.

[35] - Meirovitch, L; *Computational Methods in Structural Dynamics*; Sijthoff & Noordhof, Rockville, MD; 1980.

FIGURES

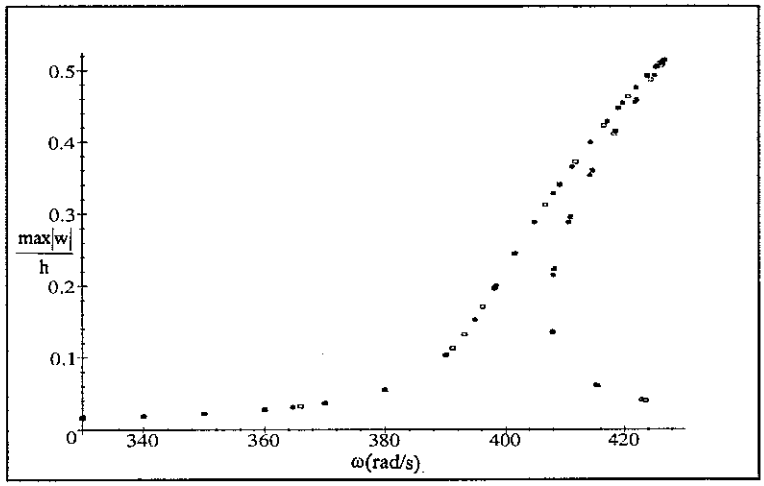

Figure 1 – FRF in the vicinity of the first mode of vibration. x=0.5×L.
o – p_o=4, p_i=4; ❑– p_o=5, p_i=5; – p_o=6, p_i=6; + – p_o=7, p_i=7.

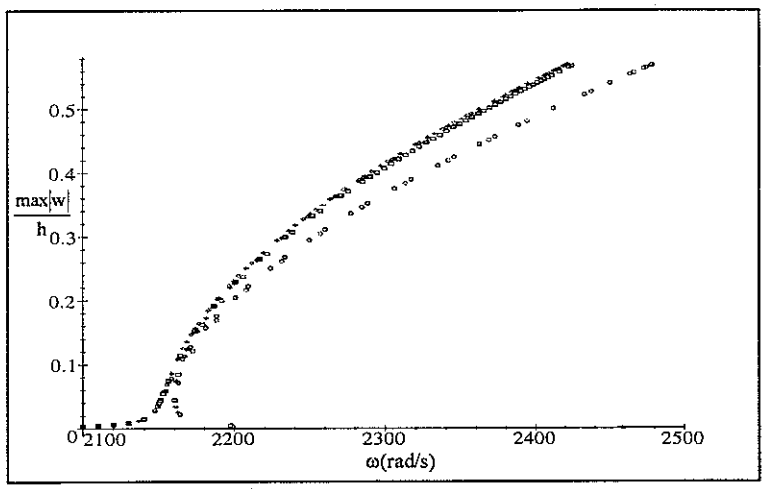

Figure 2 – FRF in the vicinity of the third mode. As above.

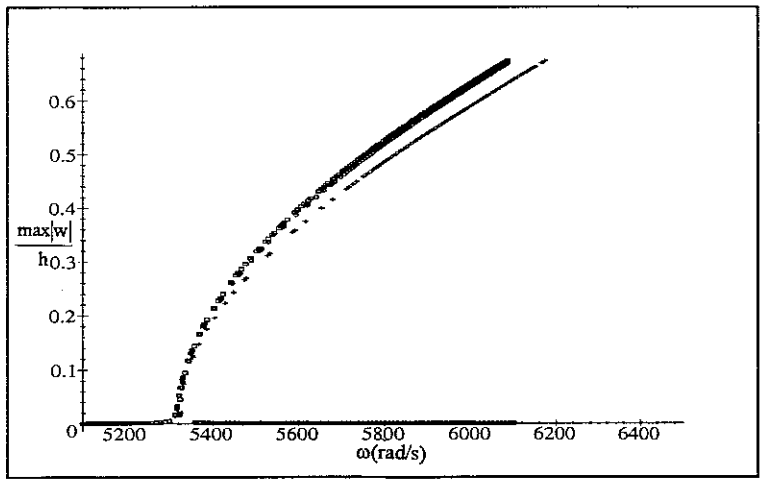

Figure 3 – FRF in the vicinity of the fifth mode. x=0.5×L.
+ – p_o=7, p_i=7; o – p_o=8, p_i=8; ❑– p_o=9, p_i=9.

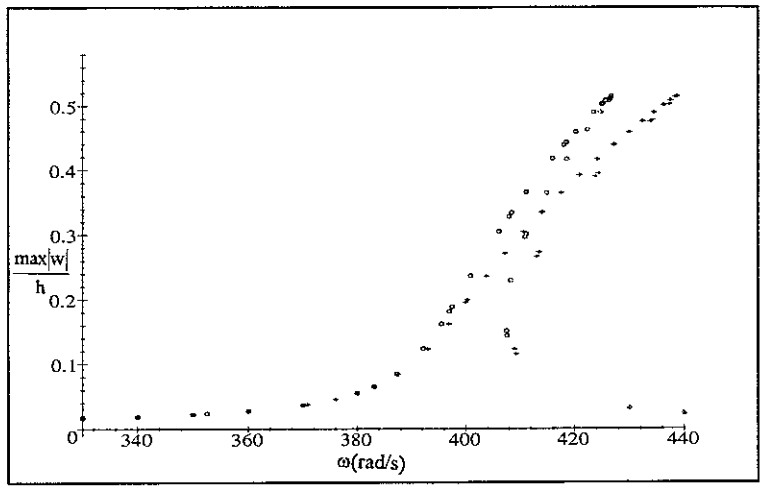

Figure 4 – FRF with in–plane displacements, p_o=6, p_i=6 (o), and without in–plane displacements, p_o=6, p_i=0 (+). x=0.5×L.

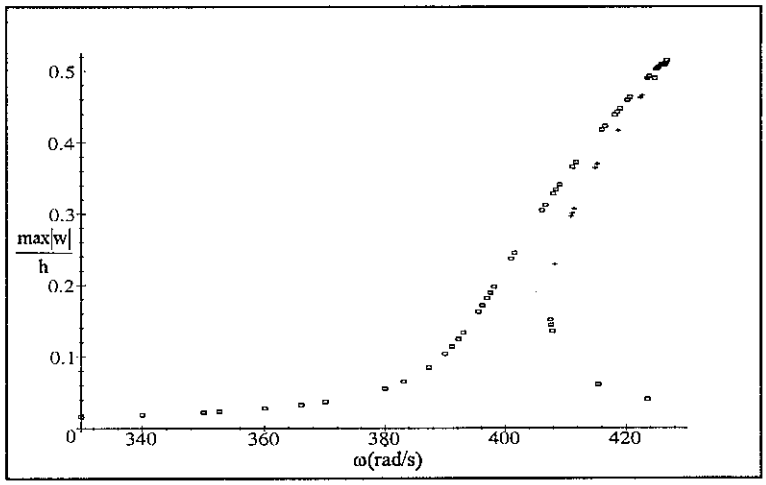

Figure 5 – Stability study using the perturbation method. First mode. x=0.5×L. ❑– stable solution; + – unstable solution; p_o=6, p_i=6.

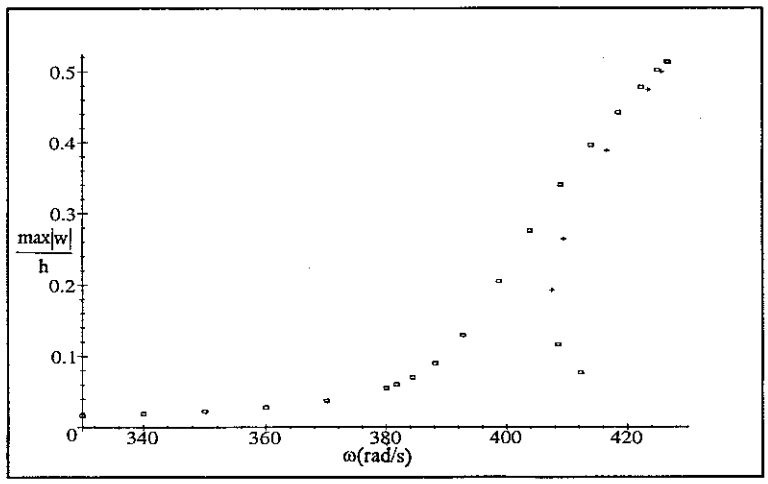

Figure 6 – Stability study, HBM with equation (3.21). First mode. x=0.5×L. ❑– stable solution; + – unstable solution; p_o=6, p_i=6.

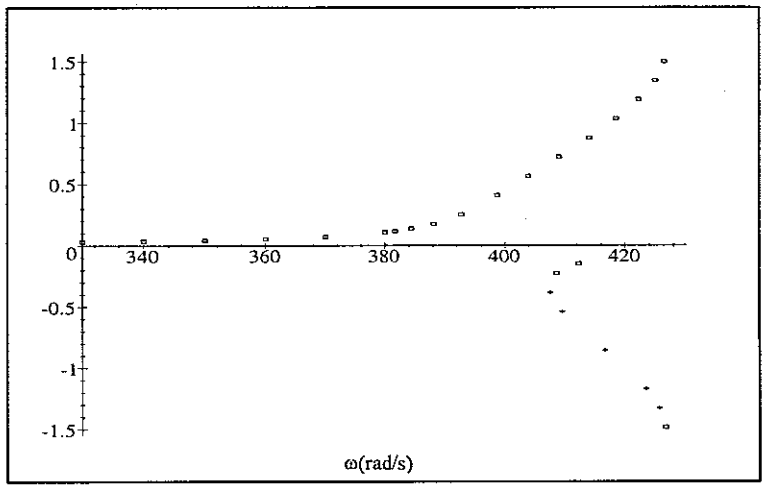

Figure 7 – Stability study, HBM with equation (3.21). First mode. x=0.5×L. ❑– stable solution; + – unstable solution; p_o=6, p_i=6.

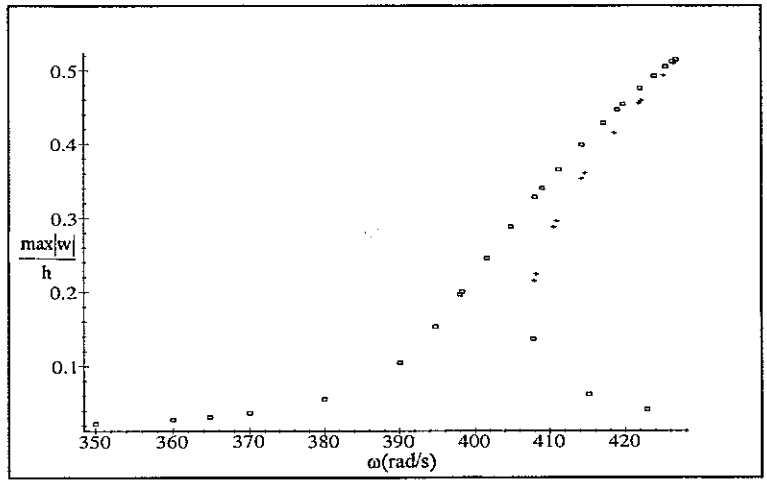

Figure 8 – Stability study, HBM with equation (3.35). First mode. x=0.5×L. ❑– stable solution; + – unstable solution; p_o=6, p_i=6.

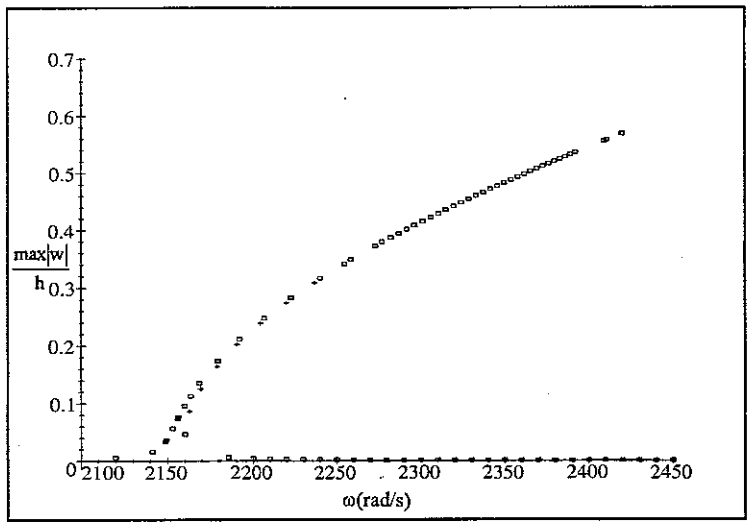

Figure 9 – Stability study, HBM with equation (3.21), k=1. Third mode. x=0.5×L. ❑– stable solution; + – unstable solution; p_o=6, p_i=6.

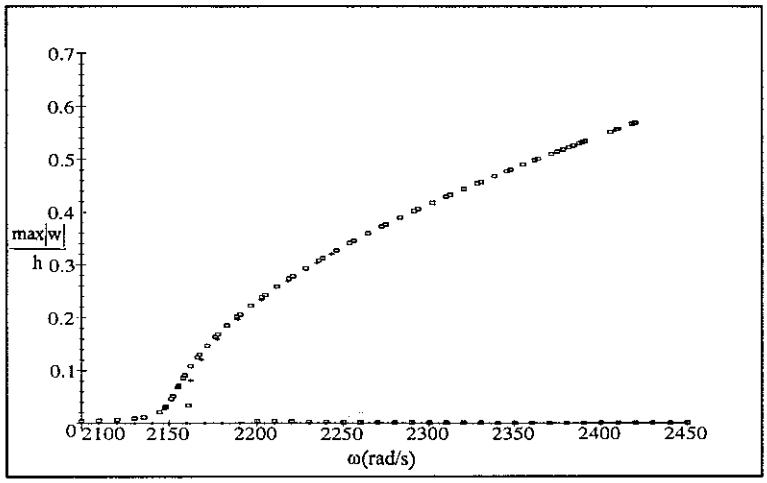

Figure 10 – Stability study, HBM with equation (3.21), k=3. Third mode. x=0.5×L.
❑– stable solution; + – unstable solution; p_o=6, p_i=6.

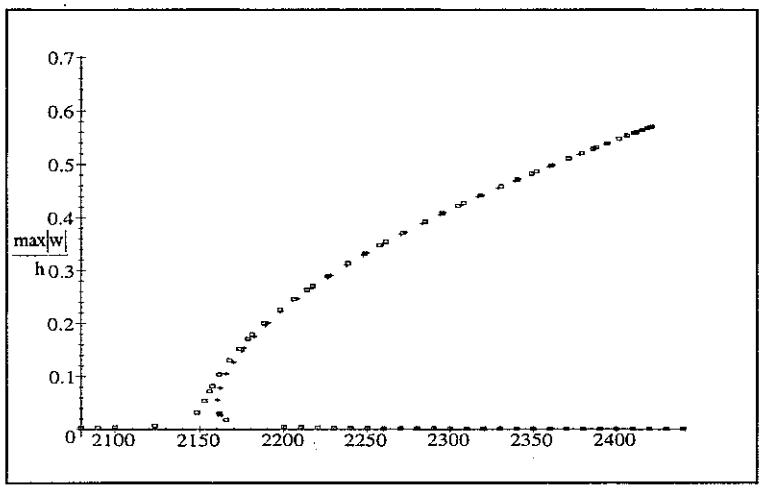

Figure 11 – Stability study, HBM with equation (3.35). Third mode. x=0.5×L.
❑– stable solution; + – unstable solution; p_o=6, p_i=6.

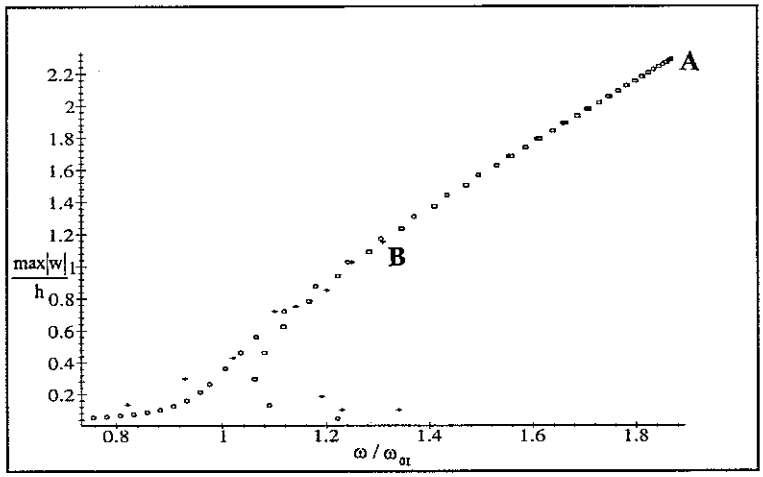

Figure 12 – Comparison with experimental results. o– HFEM stable,❑ – HFEM unstable, p_o=6 and p_i=6, β=0.01ω_{01}^2; + – experimental. x=0.5×L.

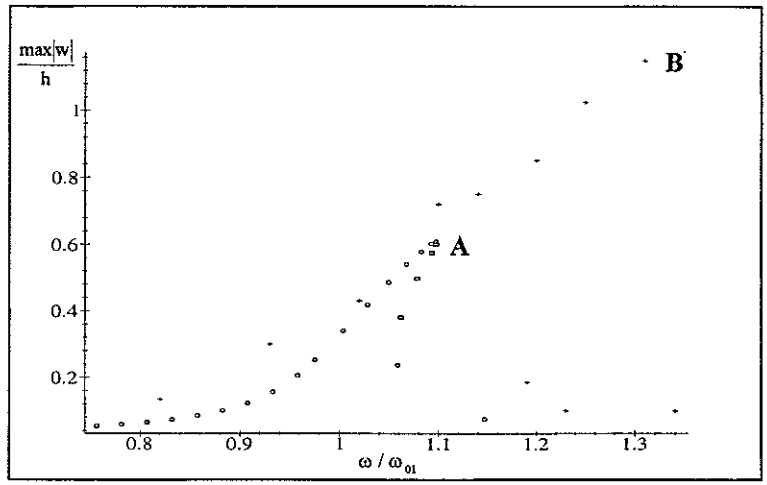

Figure 13 – Comparison with experimental results. o– HFEM stable,❑ – HFEM unstable, p_o=6 and p_i=6, β=0.038ω_{01}^2; + – experimental. x=0.5×L.

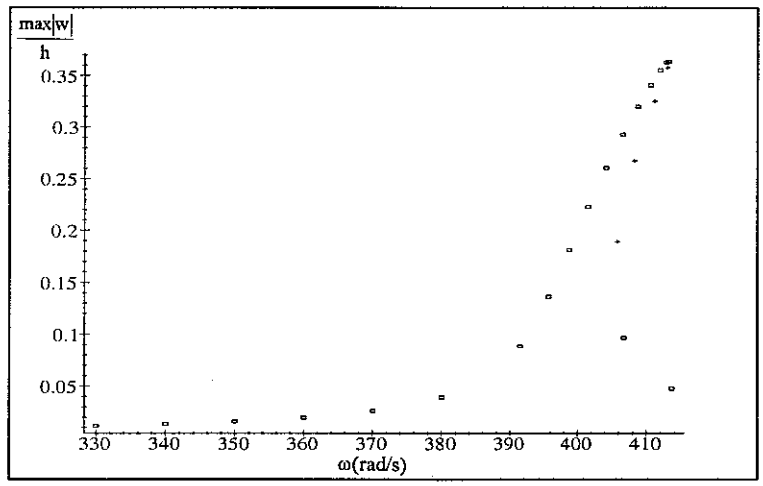

Figure 14 – FRF due to an harmonic plane wave at perpendicular incidence, first mode. ❑ – stable,+ – unstable. x=0.5×L.

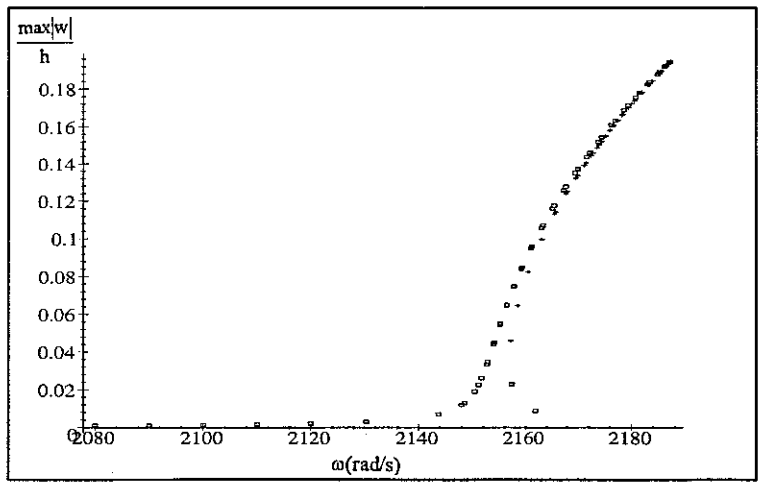

Figure 15 – FRF due to an harmonic plane wave at perpendicular incidence, third mode. ❑ – stable,+ – unstable. x=0.5×L.

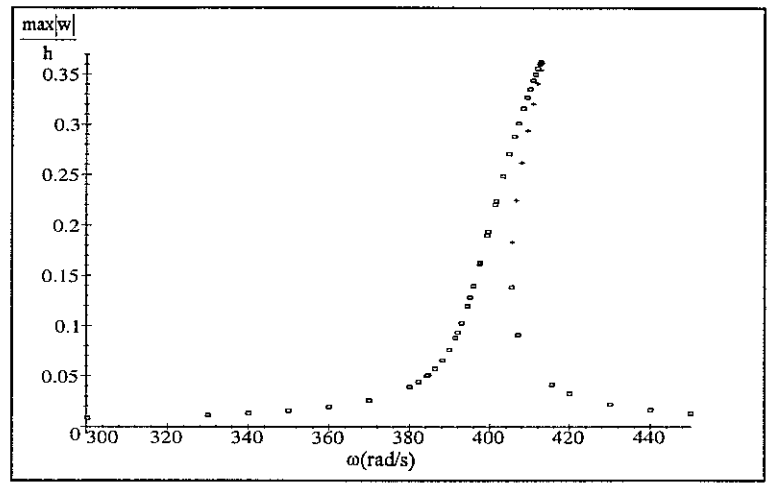

Figure 16 – FRF due to an harmonic wave at grazing incidence, first mode. ❑ – stable,+ – unstable. x=0.5×L.

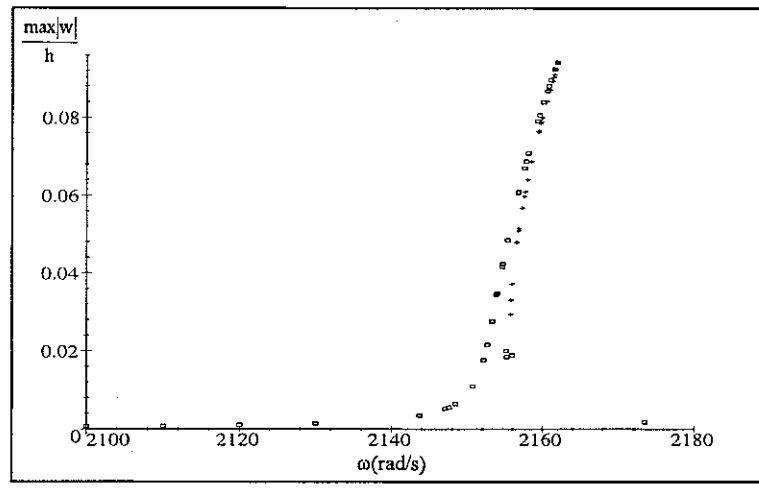

Figure 17 – FRF due to an harmonic wave at grazing incidence, second mode. ❑ – stable,+ – unstable. x=0.25×L.

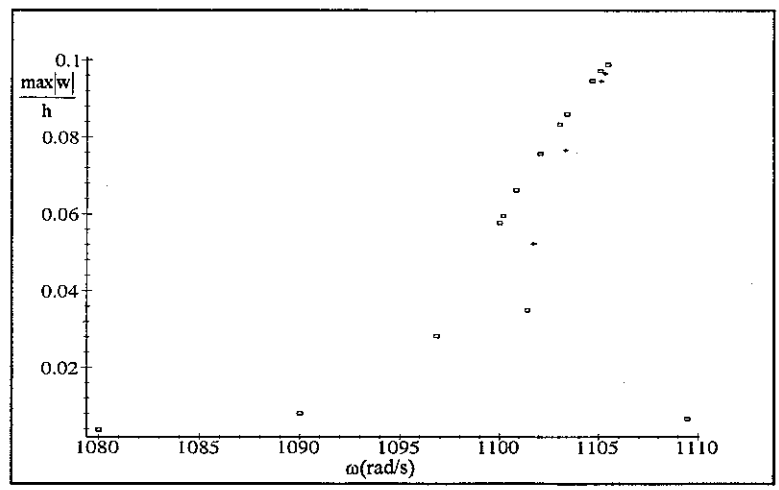

Figure 18 – FRF due to an harmonic wave at grazing incidence, third mode. ❑ – stable,+ – unstable. x=0.5×L.